The Pennsylvania State University

The Graduate School

College of Engineering

METHODS TO REDUCE DIMENSIONALITY AND IDENTIFY CANDIDATE SOLUTIONS IN MULTI-OBJECTIVE SIGNAL TIMING PROBLEMS

A Thesis in

Civil Engineering

by

Owen Hitchcock

Submitted in Partial Fulfillment

of the Requirements

for the Degree of

Master of Science

May 2018

The thesis of Owen Hitchcock was reviewed and approved* by the following:

Vikash V. Gayah

Assistant Professor of Civil Engineering

Thesis Adviser

Eric T. Donnell

Professor of Civil Engineering

S. Ilgin Guler

Assistant Professor of Civil Engineering

Patrick Fox

John A. and Harriette K. Shaw Professor

Head of the Department of Civil and Environmental Engineering

*Signatures are on file in the Graduate School

Abstract

Adjusting signal timings at signalized intersections is a practical way for transportation agencies to manage traffic without the need for significant infrastructure upgrades or additions. Traffic signal timings are directly related to the delay vehicles experience at signalized intersections. Typically, traffic engineers select signal timings to minimize the total delay experienced by vehicles at the entire intersection. At first glance, this is a fairly reasonable thing to do—minimizing the total delay at the intersection reduces the negative impacts imparted onto cars. However, there are many other possible objectives to consider when selecting signal timings at a signalized intersection. An engineer may wish to consider the approach or movement delay separately and assign a weight of importance to each. For example, one approach may experience heavy bus traffic, and thus its delay might need to be weighted more heavily to reduce the total delay experienced by all passengers served by the intersection. Or, by increasing the delay of one approach by a small amount, the delay of another approach may decrease by a large amount thus providing a more equitable distribution of delay at the intersection. These and other cases are generally not considered under current signal timing standard practice. Even when they are, no methodology exists to incorporate multiple objectives into signal timing optimization.

In light of this, the goal of this research is to develop methods that traffic engineers can use to optimize signal timings while considering multiple, potentially competing, objectives. The methods proposed rely on the application of a well-known multi-objective optimization (MOO) genetic algorithm, NSGA-II, to obtain a set of signal timings that

consider multiple objectives that may be relevant when selecting signal timings. The set of possible signal timings obtained by the MOO represents a Pareto frontier that defines the optimal tradeoffs that exist between the unique objectives. The research applies relatively new MOO visualization techniques to easily explore the tradeoffs between objectives that exist within this Pareto frontier and proposes new techniques to identify and remove objectives that might not be necessary. Additionally, methods are proposed to select the best solution in the Pareto frontier based on how a user values each of the potentially competing objectives. These methods will allow transportation agencies to obtain signal timings that provide the best tradeoff between objectives that are defined for any particular location.

Acknowledgements

First and foremost, I thank my graduate adviser and thesis committee member, Vikash V. Gayah, for guiding me through my research. I am deeply grateful for his invaluable experience, feedback, and thought-provoking questions that made my thesis possible.

I also thank my other two thesis committee members, Eric Donnell and S. Ilgin Guler, for offering their advice. The quality and thoroughness of my thesis is a testament to my committee members' dedicated time and effort.

I thank my family for always being supportive of my plans and for making the time to reunite based on my academic schedule, my friends for filling these last two years with great memories, and my professors for providing me with an excellent education.

This material is based upon work supported by the Federal Highway Administration (FHWA) under Award No. DTFH6416G00039. Any opinions, findings, and conclusions or recommendations expressed in this publication are those of the author and do not necessarily reflect the views of the FHWA.

Table of Contents

List of Tables

List of Figures

1.0 Introduction and Literature Review

1.1 Motivation

Traffic congestion in the United States is a serious issue, causing Americans to spend over 6.9 billion additional hours on the road in 2014 *(1)*. This is not only a great personal inconvenience, but the effect of urban congestion also has severe environmental and economic implications. For example, in 2014 Americans wasted 3.1 billion gallons of fuel, contributing to a congestion cost of $160 billion *(1)*. This is a problem that is likely to worsen before it improves. From 2013-2014, 95 of the 100 largest metro areas experienced an increase in traffic congestion, while only 61 did in the previous year *(1)*.

Increases in traffic congestion place a particularly heavy strain on urban areas where expanding roadway capacity by building additional infrastructure (e.g., adding lanes to existing roadways) may be impossible due to space constraints. However, modifying traffic signal timings can help to manage or decrease congestion in urban areas without the need for additional infrastructure. Changing traffic signal timings at a signalized intersection reallocates capacity among competing traffic streams, allowing a transportation agency to easily change how capacity is distributed between approaches.

Traffic signal timings are typically timed such that only a single objective, the total control delay at an intersection, is minimized *(2, 3)*. Control delay is the delay incurred by vehicles due to the presence of a traffic control device *(4)*, such as a traffic signal. This is generally a good metric to consider since reducing the total delay experienced by all vehicles using the intersection minimizes the negative impacts vehicles experience due to

the signal and allows the intersection to operate the most efficiently. However, this is a somewhat myopic perspective as there are other metrics that traffic engineers should also consider when computing signal timings, including some that may conflict with each other in unpredictable ways. These objectives include those that deal with safety, the environment, delay to other intersection users, equity, and multimodal operations. Some, if not all, of these metrics are important and may need to be simultaneously considered in the signal timing process.

Several studies have proposed multi-objective optimization (MOO) to determine optimal signal timings while accounting for multiple objectives simultaneously. In general, these methods only consider two to three objectives. These previous studies also rarely explore the relationships between the objectives in a systematic way. Specifically, these previous studies have not proposed techniques to identify and quantify the tradeoffs between the considered objectives. Finally, previous studies that have employed MOO for signal timing optimization have not provided any guidance on how to apply the results of the MOO method in practice. Most MOO procedures provide users with a large set of potential solutions that define a Pareto frontier, but obtaining a single signal timing solution to implement from this Pareto frontier is a challenging task. The proposed research will fill in the gaps present in the existing research. A detailed review of existing literature and its deficiencies are provided in the following section.

1.2 Literature Review

Previous studies in the research literature have applied several optimization methods to select signal timings while considering different potential objectives. Most

studies have only considered a single objective, but more recent studies have considered more than one objective in its signal timing optimization. These papers—and their limitations—are discussed in this section.

1.2.1 Signal timing optimization methods

Several methods have been employed to define and quantify the objectives used in signal timing optimization. Some studies use a mathematical approach to compute objectives either analytically or using mathematical models, such as the cell transmission model *(5–23)*. Other studies use simulation software packages such as VISSIM or TRANSYT-7F to quantify objectives in the optimization *(24–40)*. Optimization methods vary. When analytically possible, exact solutions to mathematical programs – such as linear and nonlinear programs – are obtained *(11, 15–19, 35)*. In many cases, however, exact solutions are not possible and heuristics such as genetic algorithms or particle swarm optimization are used to approximate the optimal solution *(5–9, 20–22, 24–34, 36–38, 41–43, 40, 23)*. These studies differ both with the specific objectives and the number of objectives considered simultaneously. Many recent studies have used genetic algorithms to optimize signal timings, particularly a non-dominated sorting genetic algorithm (NSGA-II) *(6, 23, 24, 28, 40)* that will be discussed in greater detail in Section 2.1. Regardless of the optimization method used, the process is computationally intensive and increases exponentially as the number of objectives increases. Sections 1.2.2 and 1.2.3 will describe the objectives used in previous studies.

1.2.2 Single-objective signal timing optimization

Foy et al. appears to be the first study in the research literature to optimize signal timings, minimizing the total intersection delay for its calculation ease relative to other objectives *(32)*. Zhao et al. and Wei et al. also optimized signal timings by minimizing the total intersection delay *(14, 16)*. Noaeen et al. minimized the intersection delay including shockwave effects to optimize isolated intersection cycle lengths and green splits *(17)*.

In addition to vehicle delay, some papers consider multimodal operations. Christofa and Skabardonis minimized the total person delay by considering passenger delay of passenger cars and buses when including transit signal priority in the optimization *(10)*, while Yang et al. minimized bus delay along a coordinated arterial *(5)*. Khalighi et al. minimized automobile and transit vehicle emissions to improve air quality at intersections *(18)*. Gökce et al. optimized signal timings at a large traffic circle to minimize the mean travel time, which is inherently related to vehicle delay *(37)*.

Other single-objective optimization studies also considered objectives other than delay. Fang and Elefteriadou minimized queue lengths at closely-spaced diamond interchanges to avoid queue spillback and queue storage limits *(35)*. Girianna and Benekohal maximized the throughput when optimizing traffic signals for oversaturated networks to dissipate queues as quickly as possible *(7)*. Park et al. minimized the queue time and compared it to the optimal signal timings generated from TRANSYT-7F *(30)*. Hadi and Wallace optimized signal timings to maximize progression, also using data from TRANSYT-7F simulations *(31)*.

Some studies conducted multiple single-objective optimizations to compare how signal timings might change when different objectives were considered. Leonard and Rodegerdts compared four different single-objective signal timing policies: maximizing progression and minimizing delay, number of stops, and fuel consumption *(39)*. Yun and Park separately optimized the total delay and the time vehicles spent in a queue *(29)*. Park et al. again optimized for total throughput and minimum average delay both with and without a penalty on movements with a v/c ratio above 0.9 *(33)*. Rabbani and Bullen determined green splits considering minimum total delay and equal marginal delay *(44)*. For the latter case, the delay of one additional vehicle at an approach (i.e., the marginal delay of that approach) was equalized between all intersection approaches to ensure the service at all approaches is equal.

Although a diverse set of objectives has been considered in single-objective optimization studies, real intersections are subject to many different, and potentially competing, objectives. The next section describes studies that have considered multiple objectives simultaneously in the signal timing optimization process.

1.2.3 Multi-objective signal timing optimization

The value of MOO is demonstrated because it simultaneously considers all objectives in the optimization process. Numerous studies have applied MOO to signal timing optimization. Most include two objectives in the optimizations, although some consider three or more objectives.

1.2.3.1 Papers with two objectives

Kesur minimized the total network delay and the network delay imbalance in both a fourteen-signal grid network and a nine-signal coordinated arterial network *(24)*. The network delay imbalance was determined first by calculating the average delay per foot of all possible routes through the network. The maximum value was then minimized to minimize the inequity in network delay. It was found that a small increase in total network delay corresponded to a relatively large decrease in delay imbalance. For example, a five percent increase in network delay corresponded to a 14.4 percent decrease in the arterial network delay imbalance and an 8.3 percent decrease in the grid network delay imbalance. Although this study examined delay inequity in a network, there was no measure to compare the delay inequity within approaches at an intersection.

Multiple studies considered pedestrian or bus delay simultaneously with vehicle delay. Roshandeh et al. minimized average vehicle delay and average pedestrian delay to compare crashes using these optimized signal timings with crashes using existing signal timings to determine the safety impacts of optimized signal timings *(12)*. The timings were applied to the Chicago central business district (CBD) street network using simulations to conduct a before-after analysis. The study found optimized signal timings can improve both vehicle mobility and the safety of vehicles and pedestrians. Yu et al. minimized both the vehicle delay and pedestrian delay at an intersection, considering both one- and two-stage crosswalks and their space limitations *(15)*. Although these studies considered multimodal operations in the optimizations, neither could examine the relationships between vehicle, pedestrian, and bus delay because they only included two objectives.

Some objectives—vehicle delay, number of stops, and vehicular throughput—were included in several studies. Zhang et al. minimized the total delay and maximized the traffic throughput at a set of adjacent, coordinated intersections and compared the optimized signal timings to fixed signal timings *(13)*. The study found the vehicle delay decreased up to 14.5 percent depending on the length of the connecting road, while the traffic dissipation increased up to 2.8 percent. Stevanovic et al. optimized the VISSIM performance index (PI), which includes vehicle delay and number of stops *(34)*. Although two objectives were included in the PI, the tradeoffs cannot be known because the objectives were combined into a single metric. Also, unit inconsistencies may exist between objectives in PIs, such as between number of stops and delays. A stop can be set equal to a certain length of delay, but this would be difficult to determine a priori. In a separate study, Stevanovic et al. optimized the number of vehicle conflicts and throughput *(36)*. The average delay and average number of stops were minimized to optimize the effective green time in a study by Sun et al. *(6)*. There were no comparisons to a non-optimized signal, although the study did emphasize the tradeoff between the two objectives and how an engineer can select the most appropriate solution using the Pareto frontier. In a paper by Stevanovic et al., the number of safety conflicts was minimized and the vehicular throughput was maximized along a 12-intersection arterial via simulation to compare the optimized signal timings with the initial signal timings *(26)*. A similar phenomenon found in *(24)* occurred in these findings: although the throughput remained almost the same, the number of conflicts decreased by approximately seven percent compared to the initial signal timings. Wong and Wong optimized traffic signal timings by maximizing throughput and minimizing cycle length *(19)*. Branke et al. performed two separate bi-objective optimizations,

minimizing the average vehicle delay and average pedestrian delay and later minimizing travel time and average number of stops *(28)*.

Other studies considered more non-traditional objectives in the two-objective optimizations. Zhang et al. optimized the cycle lengths, offsets, green splits, and phase sequences to minimize total delay and human exposure to pollutants in a study that found significant tradeoffs between these two objectives after applying the optimization to a stretch of roadway with five intersections *(25)*. Yin determined the optimal road toll pattern by minimizing total delay and maximizing total revenue *(21)*. Although this paper did not optimize signal timings, it provided an example of two conflicting objectives.

These bi-objective optimization problems have shown the benefits of optimizing traffic signal timings. In many cases, one objective can be greatly decreased with only minimal changes to the other. Bi-objective optimizations are advantageous because they show the relationships and tradeoffs between two objectives. However, these studies are limited by considering just two objectives at a time. Some studies have gone further and optimized for more than two objectives to gain an even greater understanding of signalized intersection operations.

1.2.3.2 Papers with more than two objectives

Aziz and Ukkusuri performed optimizations on several cases, including one that minimized total system travel time, intersection delay, and lost time *(11)*. Fang and Elefteriadou considered queue length, vehicle delay, and storage ratio (the ratio of the queue length to the available space) *(35)*. Lertworawanich et al. minimized queue spillovers and the difference in average approach delays, and maximized network

throughput *(8)*. Li et al. also considered three objectives and applied the optimized results to an intersection in Nanjing, China *(45)*. The authors examined average delay, emissions released, and fuel consumption. The optimized signal timing resulted in decreased average delay and emissions of hydrocarbons, carbon monoxide, and NO_x. Although these papers considered a more realistic number of objectives present at an intersection, they combine all objectives into one objective function. As discussed previously, the tradeoffs cannot be determined and there may be unit inconsistencies when objectives are incorporated into one objective function. The remaining studies optimized all objectives separately.

Stevanovic et al. authored a three-objective optimization paper where the three surrogate measures of mobility, safety, and environment were examined and used to optimize signals along a segment of five signalized intersections *(27)*. The objectives were to maximize throughput and minimize conflicts and fuel consumption. The study developed three-dimensional Pareto frontier surfaces and found the resulting signal timings were greatly improved from the existing timings. Chen et al. optimized signal timings for delay, stops per vehicle, and traffic capacity *(9)*.

Few studies considered more than three objectives, possibly because of the difficulty in interpreting the results as will be discussed in Section 1.3. Schmöcker et al. optimized signal timings for average car, bus, and pedestrian delays and minor- and major-street queue lengths *(20)*. Matos and Carvalho considered six objectives: control delay, trip duration, CO_2 emissions, fuel consumption, number of stops, and time lost due to driving below ideal speed *(38)*.

All of the aforementioned literature that examined traffic signal optimization—whether with one, two, or three objectives—demonstrates the potential for improving signalized intersections. However, there are several limitations or missing components with the existing literature.

1.3 Gaps in Research

Although extensive, existing literature contains two important shortcomings: there is no method to identify objectives with competing tradeoffs and there is no guidance in selecting which optimal solution is the one best solution for a certain intersection.

1.3.1 Tradeoff identification

As previously discussed, every objective has a relationship with other objectives. Some relationships may not be as important, such as an objective pair that has no tradeoff. Other relationships, such as an objective pair that does have tradeoff, are more important to the engineer. By knowing which objectives conflict with each other, and to what degree, an engineer gains a better understanding of the tradeoffs involved in the signal timing process and has the knowledge required to make a more informed decision. Furthermore, if there is little or no tradeoff between objectives, one can be removed from the optimization process to reduce the problem's dimensionality. As mentioned in Section 1.2.1, optimizations are computationally intensive so reducing the number of objectives can significantly reduce the time and computational power required. Although some existing literature *(6, 21, 26, 27)* has discussed the importance of tradeoffs and produced seemingly balanced signal timings, none have offered a method to identify or quantify tradeoffs to verify the quality of the signal timings.

1.3.2 Guidance in selecting the best solution

Every MOO results in a set of Pareto optimal solutions, which define a Pareto frontier in which one objective cannot be improved without negatively impacting another. Each solution balances the objective values differently, and it is left to the discretion of the analyst to decide what kind of balance, and therefore which solution, is most desired for the intersection. Even if the desired balance or tradeoffs are known, methods currently do not exist in the signal timing literature to identify and implement a single final solution from this set of Pareto optimal solutions. Kesur, Lertworawanich et al,. and Schmöcker et al. mention the problem of choosing a particular solution from the optimal set, but do not propose a solution *(8, 20, 24)*. As with the tradeoff identification, a method to aid a practitioner in selecting one solution from all optimal solutions would be helpful in making MOO more practice-ready.

1.3.3 Summary of research gaps

A review of existing literature found several studies discussing optimized signal timings based on one, two, or more objectives. Overall, the trend in signal timing optimization is to consider multiple objectives. In some cases, one objective can be greatly decreased while the other remains the same or only slightly increases. However, there are some deficiencies in the existing knowledge. While there are many different metrics interacting with each other at intersections, there are currently few studies that examine the interactions of more than three objectives, perhaps because it is so difficult to interpret the results. Also, few studies considered objectives such as inequity and multimodal operations, and many papers combined multiple objectives into one objective function.

MOO studies that investigated the relationships between multiple objectives have not offered a way to identify and quantify the tradeoffs between competing objectives. Finally, there has been no guidance for a practitioner to select the best optimized solution. This research proposes to fill these voids in the existing literature.

1.4 Research Objectives

The major research objectives alluded to above are to:

1) use MOO for many different objectives to determine signal timings that consider more than just two or three objectives simultaneously;
2) propose methods to identify and quantify the tradeoffs between objectives to help remove objectives that might be redundant; and,
3) develop a methodology to provide guidance in selecting a signal timing plan that selects the best balance between all objectives.

2.0 Methodology

2.1 Multi-objective Optimization Algorithm

This research will use a MOO algorithm that was implemented in MATLAB. The algorithm is the second version of a non-dominated sorting genetic algorithm, called NSGA-II *(46)*. Genetic algorithms have been used in various traffic engineering papers as early as 1992 *(7, 22, 32)* but have seldom been utilized until recently due to their computational demand *(27)*. As a type of evolutionary algorithm, a genetic algorithm ultimately results in solutions, or sets of decision variables, that minimize or maximize objectives while satisfying constraints. First, the user inputs the amount of solutions to output and generations to run. The user also inputs the objectives to minimize or maximize, as well as the constraints. With these inputs, the algorithm first chooses a random set of initial solutions, which correspond to a set of initial objective values. The decision variables are randomly changed with each generation, and these changes are kept if the objectives are improved. After many generations, each solution converges to an optimal solution in which it is not possible to improve one objective without sacrificing another. The set of these optimal solutions is referred to as the Pareto frontier. All solutions in the Pareto frontier are equally optimal in the absence of any additional user-provided information based on their preferences. An example of a Pareto frontier is shown in Figure 1.

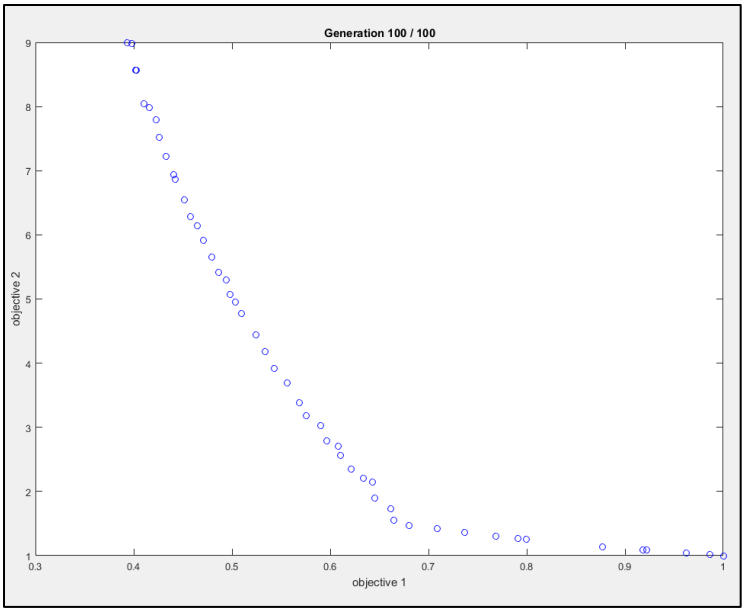

Figure 1: Example of a Pareto frontier

Figure 1 shows that any solution to the right of the frontier can be improved by decreasing one or both objective values. The number of solutions considered in the MOO process defines the precision at which the Pareto frontier can be determined: more solutions means a more precise definition of the Pareto frontier. As mentioned earlier, each generation brings the initial solutions closer to the Pareto optimal solutions. Therefore, a higher number of generations increases the likelihood of converging to the Pareto frontier. Users should use a high number of solutions and generations to reveal the true Pareto frontier, although this increases the computational cost due to the increased algorithm run time.

A very recent update to NSGA-II was created and is known as NSGA-III *(47)*. This algorithm is optimized for many-objective optimizations, or optimizations with more than four objectives. However, NSGA-II has a longer history and has been more widely-used. Furthermore, Matos and Carvalho found that NSGA-II outperformed NSGA-III in a many-

objective traffic signal timing optimization *(38)*. Finally, the main purposes of this research are to explore many different objectives, introduce a tradeoff visualization and identification technique, and propose methods for selecting the best solution from a set of solutions. Because the exact algorithm used is not crucial for these purposes, this research uses the more widely-used NSGA-II algorithm. For more detailed information about the this algorithm, the reader is encouraged to consult the original paper proposing NSGA-II *(46)*.

2.2 Tradeoff Index and Mosaic Plot

As described in Chapter 1, a major shortcoming of existing traffic engineering literature is that there have not been any methods to identify tradeoffs that exist between competing objectives in multi-objective signal timing optimization. Researchers can speculate which objectives may logically conflict with each other, but there is no way to quantify the tradeoffs and know whether or not these tradeoffs actually exist.

This research proposes the introduction of the newly-developed mosaic plot into the traffic engineering research field. The mosaic plot, developed by Unal et al. in 2015 *(48)*, improves upon existing methods of identifying tradeoffs between many objectives. Prior to the development of the mosaic plot, the two most common tradeoff identification techniques were the scatter plot matrix and parallel coordinate plot *(48)*, both of which are shown in Figure 2. The scatter plot matrix shows all the two-dimensional Pareto frontiers between all objective pairs. As the number of objectives increases, the number of sub-matrices required to show all relationships also rapidly increases. The parallel coordinate plot displays the objective values of each solution as a single line. The crossing of one line

over another indicates a tradeoff between the two objectives, and a higher number of crossing lines indicates a higher tradeoff. As the number of objectives increases, usage of the parallel coordinate plot requires many different figures to observe the tradeoff between every unique pair of objectives.

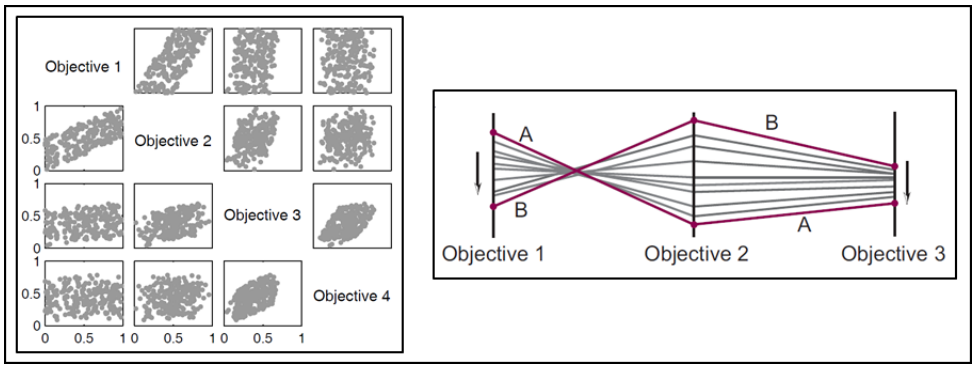

Figure 2: Scatter plot matrix and parallel coordinate plot *(48)*

In contrast to these two methods, the mosaic plot only requires one reasonably-sized figure and allows the user to quickly determine the relationship between each objective pair. The key component to the mosaic plot is the tradeoff index, which quantifies the degree of tradeoff between a pair of objectives. The tradeoff index is defined as:

$$\lambda_{i,kl} = \frac{\sum_{j=1}^{N_{sol}} \beta_{ij,kl}}{N_{sol}-1}, j \neq i \quad (1)$$

where:

N_{sol}: number of solutions; and,

$\beta_{ij,kl}$: binary factor if *i*th and *j*th solutions cross between objectives *k* and *l*.

The binary factor $\beta_{ij,kl}$ is equal to zero if the solutions do not cross and one if the solutions do cross. As shown above, the tradeoff index of Solution *i* is an average of ones and zeros depending on the number of times the Solution *i*''s line segment crosses other solution line

segments. The tradeoff index is bounded to $\lambda_{i,kl} \in [0,1]$, with values near zero indicating lower tradeoffs and values near one indicating higher tradeoffs. With the tradeoff index of all solutions, the homogenized tradeoff index Λ_{kl} can be calculated to determine the average tradeoff between Objectives *k* and *l* for all solutions:

$$\Lambda_{kl} = \frac{\sum_{i=1}^{N_{sol}} \lambda_{i,kl}}{N_{sol}} \quad (2)$$

This results in the average value of all tradeoff indices between objectives *k* and *l*, representing the average tradeoff between the two objectives. Using this measure, the tradeoff between objective pairs can be quantified. These tradeoff indices are also used to create the mosaic plot visualization technique.

Tradeoffs are color-coded, with white representing no tradeoff, black representing complete tradeoff, and varying shades of gray to represent all levels in between. A darker gray represents higher tradeoff between two objectives. Example mosaic plots are shown in Figure 3.

a)

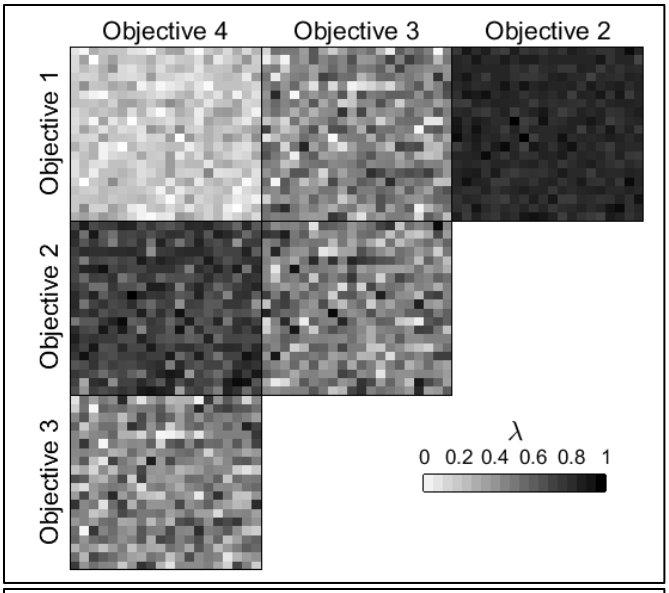

b)

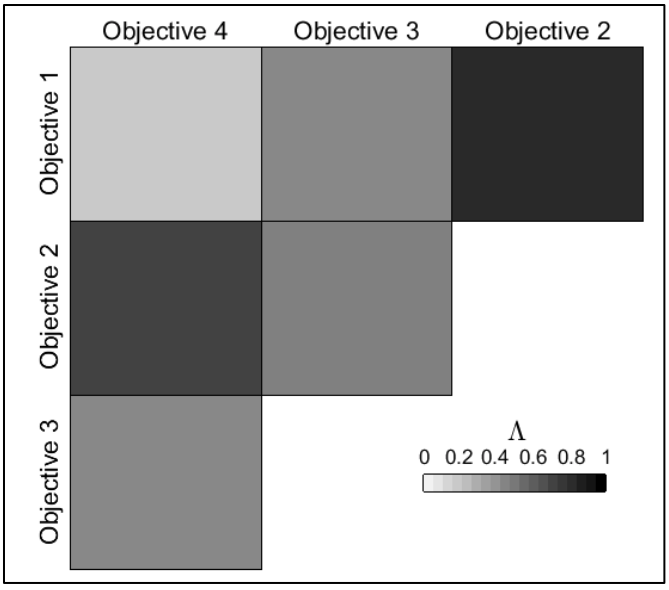

Figure 3a) Mosaic plot, and b) homogenized mosaic plot *(49)*

In Figure 3a, the small individual squares show the tradeoff of every solution, or the tradeoff index λ. The homogenized mosaic plot in Figure 3b is obtained by computing the average tradeoff of all solutions, or the homogenized tradeoff index Λ. In the above example, Objective 1 and Objective 2 have the highest tradeoff because their intersecting square is the darkest. Likewise, Objectives 1 and 4 have the lowest tradeoff because that square is the lightest. In the mosaic plot creation process, the calculated tradeoff indices

are saved if the user desires to more accurately compare tradeoffs rather than visually estimating them. It can be seen that if a fifth objective were added to Figure 3, the mosaic plot would slightly grow in size to compare all possible objective pairs, but no additional plots would be required (unlike the parallel coordinate plot and scatter plot approaches).

This research will use the mosaic plot to easily illustrate the tradeoffs between competing objective pairs. If one objective is determined to be non-competing with all other objectives, this non-competing objective can be removed to reduce the dimensionality of the problem and ensure two similar objectives do not influence the solutions in a biased manner. This is described in further detail in the next section.

To determine if an objective is non-competing, the average homogenized tradeoff index δ_k is proposed here. This index is simply the mean of all homogenized tradeoff indices for a given objective value. It represents the overall relationship an objective has with all other objectives. Like the individual objective tradeoff indices, the higher the value, the greater the tradeoff. The average homogenized tradeoff index is defined as:

$$\delta_k = \frac{\sum_{m}^{M-1} \Lambda_{km}}{M-1}, k \neq m \tag{3}$$

where

Λ_{km}: homogenized tradeoff between Objective *k* and Objective *m*

M: number of objectives

Once the optimal solutions are generated by the MOO algorithm and the mosaic plots are created, the next step is to identify and remove redundant objectives.

2.3 Redundant Objective Identification

The above indices can determine if an objective is redundant and if so, it can be removed from the MOO and a new iteration of the MOO process can be performed. Only one objective is removed per iteration. This process continues and stops when there are no more redundant objectives in an iteration. The practitioner will then select solutions from this final iteration.

There are several reasons why removing redundant objectives is desirable. The most applicable reason to practitioners is computational efficiency. MOOs with many objectives require more powerful computers or more time to run. By decreasing the number of objectives, the optimization can be completed more quickly. While this requires more work initially, the redundant objective results can be used for similar intersections or the next time MOO is used for the intersection. Another reason to remove redundant objectives is because it increases the likelihood of finding the Pareto optimal solution within the given number of generations. Each objective corresponds to one dimension in the solution space, so the space increases as the number of objectives increases. Finding the Pareto optimal solution is less likely when the space is large. By removing redundant objectives and decreasing the size of the space, the solutions become denser and the MOO has a higher chance of finding the Pareto optimal solution. Finally, practitioners may choose to remove two correlating objectives simply due to their redundancy so the MOO does not take two similar objectives into consideration. An example of this will be provided in Chapter 3, which provides a numerical example demonstrating the methodology.

There are two methods to determine if objectives are redundant. One method is to use the average homogenized tradeoff index, or δ_k, described in the previous section. Practitioners may set a minimum acceptable value for δ_k and if an objective is less than this value, it is removed. The procedure for determining this value can be as simple as assigning a value (for example, 0.3) or some other more involved process. Another way to identify redundant objectives is to compare the respective tradeoff indices of two objectives with the remaining objectives. If the tradeoff indices between the remaining objectives and the two objectives are similar and the two objectives do not trade off significantly with each other, one of them can be removed. For example, if Objectives *k* and *l* have respective tradeoffs of 0.55 and 0.54 with Objective *a*, 0.38 and 0.37 with Objective *b*, and 0.62 and 0.63 with Objective *c*, either Objective *k* or *l* can be considered redundant (provided they have low tradeoff with each other) because their tradeoffs with the remaining objectives are similar. As with the other objective redundancy identification method, the definition of similar is chosen by the practitioner. In this example, the absolute difference was 0.01 for each remaining objective but a practitioner can choose their threshold values for redundancy.

If the above procedures are followed, a practitioner will identify a redundant objective in the MOO to remove. However, the results may conflict with the desire of transportation agencies. For example, a practitioner may conclude that a certain objective should be removed but if an agency requires that objective to always be included, the second most redundant objective can be removed. While the above procedures are guidelines for identifying redundant objectives, they are not strict standards. Practitioners

may follow these guidelines as closely as they desire depending on the agency's mandates. In the absence of such mandates, these guidelines should be followed.

2.4 Methods for Selecting Best Solution

As mentioned earlier, the MOO will output as many optimal solutions as the user specifies, which should be a large number in order to precisely define the Pareto frontier and maximize the probability of finding the best solution for an intersection. With these MOO-generated optimal solutions, the user will need to apply their own judgement to subjectively pick one solution that works best for an intersection. To do so, the user will require a method to select the best of the optimal solutions.

A mathematically sound method is required to fairly rank all solutions so that all objectives are weighted equally. For example, simply summing the objective values and using the minimum sum as the best solution would result in a biased solution because objectives with larger values will have a greater effect on the sum. Also, objectives have different units that cannot be added together. For example, there is no logical meaning to the sum of stops and delay because stops and vehicle-seconds cannot be added. As mentioned earlier, it would be difficult to set one stop equal to a certain length of delay a priori. This is a drawback of approaches that combine multiple objectives into one single objectives. In order for a fair comparison to be made, objective values must be compared to other objective values of the same magnitude and units.

In this research, two methods are proposed to help a user sort through the solutions and identify the one(s) that provide the best balance between the competing objectives. The

methods are described using the objective value ratio θ_{ik} and ratio product Θ_i, as proposed below.

2.4.1 Method 1

In Method 1, all solutions are ranked based on their objective value ratio to the minimum objective value. Since all objectives are to be minimized (maximized objectives can be multiplied by -1 and then minimized), the best solution will have relatively low objective values for all objectives. For each objective value of each solution, the objective value ratio is defined as:

$$\theta_{ik} = \frac{OV_{ik}}{\min\limits_{i}(OV_{ik})} \tag{4}$$

where:

OV_{ik}: Solution *i*'s value for Objective *k*

Every solution *i* will have an objective value ratio for each objective *k* and $\theta_{ik} \geq 1$. For each solution, all objective value ratios are then multiplied together to obtain the ratio product:

$$\Theta_i = \prod_{k=1}^{M} {\theta_{ik}}^{w_k} \tag{5}$$

where:

M: number of objectives

w_k: weighting factor for Objective *k*

The decision-maker may assign weighting factors to objectives they deem more important, which is helpful if a decision-maker or agency wishes to prioritize one or more objectives. The objective value is raised to w_k rather than multiplied to ensure w_k is applied to the desired objective. If it were multiplied, the commutative property would cause w_k to be applied to the product of all objective values and not be specific to one objective, essentially rendering it useless. Calculation of w_k is dependent on the decision-maker. They may use a relatively arbitrary number (e.g., three to denote an objective as three times more important) or they may create a more complex definition process. To weigh all objectives equally, each weighting factor is set to one. Solutions with lower θ_{ik} have lower deviations from the minimum objective value; a solution with an θ_{ik} equal to one indicates the solution has the lowest value for the corresponding objective. Continuing with this logic, a solution with a Θ_i closer to one has the fewest differences from minimum objective values. Therefore, all the ratio products for each solution are sorted in ascending order to determine which objectives from among the solutions are closest to the minimum value. The highest-ranked solution is labelled the best solution, as it does the best job at simultaneously minimizing all objective values.

2.4.2 Method 2

The process for Method 2 is similar to Method 1, but uses a constrained set of solutions instead of all solutions in the Pareto frontier set. Decision-makers establish a maximum value for one or more desired objectives and then add a constraint in the optimization such that no objective values exceed the criteria. After the optimization is ran and a new set of constrained solutions is created, the process follows similar steps as

Method 1. The only difference is the calculation of Θ_i. The objective value ratio for the constrained objective is not included in this calculation because its effect on Θ_i was already taken into account with the added constraint. For Method 2, Θ_i is defined as:

$$\Theta_i = \prod_{k=1}^{M} \theta_{ik} \ , k \neq m \tag{6}$$

where

m: filtered objective

This method would be used if a decision-maker or agency requires a maximum acceptable objective value for one or more objectives.

3.0 Numerical Example

A fictional intersection will be used to demonstrate the methodology described in the previous chapter. This fictional example was used for its simplicity in order to focus on relationships between the objectives, which are described below. It is noted that the purpose of this example is to demonstrate the methods; the intersection properties and objectives here are not crucial for the methodology.

3.1 Setup and Objectives Used

Signal timings were optimized for a pre-timed signalized intersection with the following characteristics:

- Isolated
- Under-saturated
- Four two-way approaches
- Protected or permitted left turns
- Four pedestrian crosswalks
- Uniform vehicle and pedestrian arrivals

The geometry, lane group vehicle volumes, and crosswalk pedestrian volumes are shown in Figure 4, and the phase sequence diagram is shown in Figure 5.

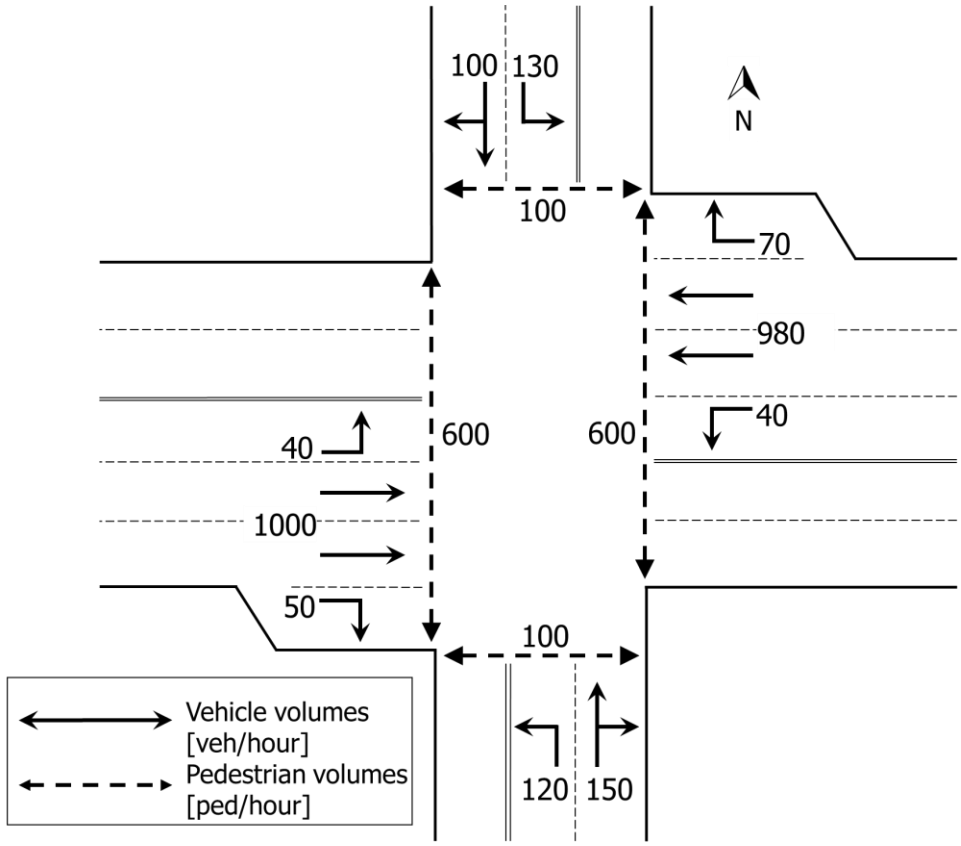

Figure 4: Isolated intersection example

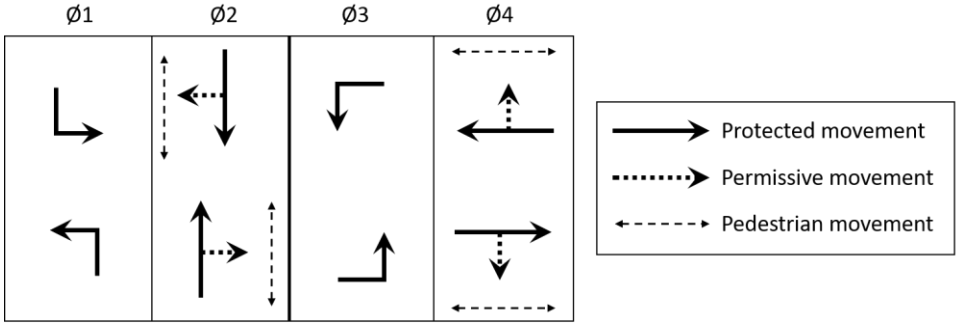

Figure 5: Isolated intersection phase sequence

There was no constraint on the cycle length. Additionally, there were two types of left turn treatments tested: protected and permitted. The east-west (EW) left turns were assumed to always have a protected left turn phase but the north-south (NS) left turns were assumed to be protected in one case and permitted in another to demonstrate that this

method can be applied in either situation. The assumed signal timing information is shown in Table 1.

Table 1: Traffic signal characteristics

Variable	Value
Cycle length	Variable
Left turn minimum green times	2 seconds
Left turn maximum green times	60 seconds
Thru/right minimum green times	19.1 seconds (NS); 9.6 seconds (EW)
Thru/right maximum green times	60 seconds
Yellow time	3 seconds
All-red time	1 second
Lost time per cycle	16 seconds

The minimum green times were calculated using the 2010 HCM Equation 31-72 to allow sufficient pedestrian crossing time while assuming eleven-foot lanes, a pedestrian walking speed of 3.5 feet per second, and the use of the yellow phase for pedestrian crossing. All lane group occupancies were 1.1 passengers/veh, with the exception of the Northbound left which had an average occupancy of 1.5 passengers/veh to model an approach with heavy bus traffic. The base saturation flow was 1700 veh/hr/lane, with right- and left-turn adjustments made in accordance with Equations 18-10 and 18-11 in the 2010 HCM *(4)*. Again, it is noted these intersection properties were chosen for simplicity.

Six objectives were used in the MOO. These objectives were chosen because of their novelty, applicability, and ability to be analytically quantified (e.g. not derived from simulations). However, the ranking methodology does not require these objective characteristics—if desired, objectives may be obtained through other methods such as simulation or the use of a mathematical model. As long as the final generation of MOO solutions are provided, the ranking methods will work. All objective values are computed

for a one hour period and are minimized. Objective value calculations for permitted and protected left turns were the same for all objectives except for the total number of stops as noted in Section 3.1.5.

3.1.1 Total intersection vehicle delay

The first objective considered is the total intersection vehicle delay, which is the primary objective that is currently considered when timing traffic signals according to the research literature *(2, 3)*. The total intersection vehicle delay represents the total delay experienced by all vehicles traveling through the intersection during the one-hour analysis period considered. For the purposes of this research, vehicle delays are estimated using the methodology contained in the 2010 edition of the *Highway Capacity Manual* (HCM) *(4)*. Since only under-saturated conditions are considered, the delay for each lane group at the intersection is equal to the sum of two components: uniform delay and incremental delay. Uniform delay is the average delay vehicles will experience under the assumption that they arrive at a constant rate, while incremental delay accounts for the random periods during which demand exceeds capacity and the intersection is temporarily oversaturated. The average uniform and incremental delay per vehicle for any individual lane group, d_i, is calculated from Equation 31-159 from the 2010 HCM:

$$d_i = \left(\frac{PF*0.5*C*\left(1-\left(\frac{g}{C}\right)_i\right)^2}{1-\left[min(1,X_i)*\left(\frac{g}{C}\right)_i\right]}\right) + \left[900 * T * \left[(X_i - 1) + \sqrt{(X_i-1)^2 + \frac{8*k*I*X_i}{c*T}}\right]\right] \quad (7)$$

$$C = \sum_i^N g_i + lost\ time \quad (8)$$

where

d_i: average delay per vehicle [seconds/vehicle]

N: number of lane groups

c: capacity [vehicles/hour]

g_i: green time for Lane Group *i* [seconds]

I: adjustment factor for upstream filtering/metering [1 for isolated intersections]

k: adjustment factor for controller type [0.5 for pretimed controllers]

PF: progression factor [1 for uncoordinated intersections]

T: analysis period [1 hour]

X_i: volume/capacity (v/c) ratio for Lane Group *i*

V_i: vehicle volume for Lane Group *i* [vehicles/hour]

The first part of the above equation represents the uniform delay component while the second part represents the incremental delay component.

The total intersection vehicle delay, D_v, is simply the weighted sum of the average delay per vehicle, using the hourly volumes as the individual weights:

$$D_v = \sum_{i=1}^{N} d_i * V_i \quad (9)$$

where

D_v: total vehicle delay [vehicle-seconds]

3.1.2 Vehicle delay inequity

Vehicle delay inequity quantifies the fairness of vehicle delays experienced by individual lane groups compared to the others. The vehicle delay is used to compute the difference between the maximum average delay experienced by any lane group and the

minimum average delay experienced by any lane group. A larger difference indicates a more unequal distribution of delays. Not only is a large inequity unfair, but drivers may be more likely to perform illegal maneuvers if they perceive their delay to be unequal. This objective is defined as:

$$ineq_{veh} = \max(d_i \; \forall \; i) - \min(d_i \; \forall \; i) \tag{10}$$

with all variables defined previously.

This objective is important to consider because a lower objective value creates an intersection where delays are distributed more equitably across approaches. By including vehicle delay inequity in the MOO, the overall tradeoffs between lane group delays can be expected to decrease. For example, if a solution causes the average delay of one lane group to increase by five seconds while another lane group delay decreases by thirty seconds, the solution can be considered more equal. Even though the average delay increased for one lane group, the other lane group average delay decreased by a much larger amount.

3.1.3 Total intersection passenger delay

The total intersection vehicle delay objective is a useful metric but fails to consider passenger occupancies in each vehicle. In reality, lane groups can have different average occupancies, particularly lane groups with heavy higher-occupancy public transportation traffic. Total intersection passenger delay is a better objective when considering intersections and lane groups with higher-occupancy vehicles, such as buses—even though a bus is only one vehicle, this objective prioritizes buses because of its higher average occupancy. Because buses typically have a higher occupancy, reducing the bus delay decreases the passenger delay more than by reducing the vehicle delay, which includes

lower-occupancy vehicles. The total intersection passenger delay is based on the total intersection vehicle delay and the average vehicle delay estimation methodology. The difference here is that each lane group delay is multiplied by its average occupancy to obtain the total passenger delay in units of passenger-seconds:

$$D_p = \sum_{i=1}^{N} d_i * V_i * occ_i \quad (11)$$

where

D_p: total passenger delay [passenger-seconds]

occ_i: average vehicle occupancy [passengers/vehicle]

3.1.4 Passenger delay inequity

Passenger delay inequity is considered to incorporate vehicle occupancies into the inequity calculations. Again, the inequity is defined as the difference between the maximum average passenger delay and the minimum average passenger delay. The larger the difference, the more unequal the intersection is. Passenger delay inequity is defined as:

$$ineq_{veh} = \max(d_i \times occ_i \; \forall \; i) - \min(d_i \; \times occ_i \; \forall \; i) \quad (12)$$

where

$ineq_{veh}$: vehicle delay inequity [seconds]

3.1.5 Total number of stops

The total number of stops per cycle is an important metric because it has safety, environmental, and economic impacts. A higher number of vehicles stopping increases the opportunities for rear-end collisions. Also, a vehicle idling or accelerating from a stop

releases more emissions than cruising through an intersection without stopping or decelerating. Finally, stopping and decelerating at intersections increases both user and agency costs. Increased braking wears out vehicle brake pads earlier, and decelerating heavy vehicles can cause longitudinal rutting on flexible pavements. The number of stops per hour can be analytically estimated using queuing theory as *(50)*:

$$n_i = \sum_{i=1}^{N} \frac{V_i * S_i * (C - g_L)}{C * (S_i - V_i)} \quad (13)$$

where

n_i: number of stops per hour in Lane Group *i* [vehicles]

S_i: saturation flow of Lane Group *i* [vehicles/hour]

g_L: g_i for protected left turns [seconds]

g_U (green time unblocked by opposing vehicles) for permitted left turns [seconds]

As stated earlier, the above equation assumes a uniform demand and an under-saturated intersection.

3.1.6 Total crosswalk pedestrian delay

Previous objectives focused on vehicles and passengers of vehicles. At urban intersections, it is also important to consider the needs of pedestrians. Therefore, the total delay pedestrians experience waiting to cross on crosswalks is another objective to consider. It is important to consider the pedestrian delay because if pedestrians experience a high delay, they may become impatient and cross the street illegally, creating a safety hazard for both themselves and motorists. The individual delay experienced at each street crossing is estimated using the 2010 HCM Equations 18-49 and 18-71 *(4)*:

$$d_{ped,j} = \frac{0.5(C-g_o+4.0)^2}{C} \quad (14)$$

where

j: crosswalk group

$d_{ped,j}$: average delay per pedestrian [seconds/pedestrian]

g_o: vehicular cross-traffic green time [seconds]

The addition of four seconds to the cross-traffic green time represents an addition to the pedestrian effective walk time caused by pedestrians entering the intersection in the first four seconds of the pedestrian clear interval *(4)*. As with vehicle delay, the individual crosswalk delay is then weighted by the hourly pedestrian volumes. The total pedestrian delay on crosswalks is an objective defined as:

$$D_{ped} = \sum_{j=1}^{M} d_{ped,j} * V_{ped,j} \quad (15)$$

where

D_{ped}: total pedestrian delay [pedestrian-seconds]

M: number of crosswalks

V_{ped}: pedestrian volume [pedestrians/hour]

Including this objective ensures the intersection signal timing considers pedestrians in addition to vehicles.

The results of optimizing signal timings for the above intersection, constraints, and objectives are discussed in the next two sections.

3.2 Single-objective Optimization Results

First, the results of single-objective optimization (SOO) are shown to demonstrate the need for multi-objective optimization. First, the results from the protected left turns (protected LT) intersection are discussed. Then, the results from the permitted left turns (permitted LT) intersection are discussed.

3.2.1 Protected left turns

The single-objective optimized green times for protected LT are provided in Table 2 and the ranges are shown in Table 3.

Table 2: Single-objective optimized green times (protected LT)

Minimized objective	NS L green (sec)	NS T/R green (sec)	EW L green (sec)	EW T/R green (sec)	Cycle length (sec)
Total vehicle delay	10.7	19.1	4.1	43.0	92.9
Vehicle delay inequity	18.6	19.1	13.0	34.1	100.8
Total passenger delay	11.0	19.1	4.1	41.9	92.1
Passenger delay inequity	20.0	19.1	7.7	29.9	92.8
Total number of stops	8.7	19.1	2.7	60.0	106.5
Total pedestrian delay	6.5	19.1	2.0	35.5	79.1
Note: “L” denotes the left turn green time and “T/R” denotes the thru/right turn green time					

Table 3: Range in single-objective optimized green times (protected LT)

NS L range (sec)	NS T/R range (sec)	EW L range (sec)	EW T/R range (sec)	Cycle length range (sec)
13.5	0.0	11.0	30.1	27.4

The cycle length and each green time greatly varies when minimizing for one objective compared to minimizing for the other objectives. The large range in single-objective minimized green times for each approach demonstrates the need to optimize for multiple objectives. If the green times had a small range (e.g. all green times were very similar), it would not be necessary to consider multiple objectives during the optimization

because optimizing for any one objective would also optimize all other objectives. However, the large range indicates each objective requires a different green time to be minimized. For example, optimizing for passenger delay inequity requires 20.0 seconds of NS L green time. If vehicle delay is instead optimized, the resulting green time is 10.7 seconds. This would likely result in a large vehicle delay inequity objective value. While the cycle length and most approaches have a large range, the NS T/R green time does not have a large range. This is because all values are the minimum green time to allow sufficient pedestrian crossing time. If this constraint was not imposed, the NS T/R green times would likely also display a large range. The objective values resulting from SOO also vary greatly, as shown in Table 4 and Table 5. Minimum objective values are bolded.

Table 4: Single-objective optimized objective values (protected LT)

Minimized Objective	Objective Value					
	Total vehicle delay (veh-sec)	**Vehicle delay inequity (sec)**	**Total passenger delay (pass-sec)**	**Passenger delay inequity (sec)**	**Total number of stops (vehs)**	**Total pedestrian delay (ped-sec)**
Total vehicle delay	**72,320**	59	82,240	68	2,103	18,896
Vehicle delay inequity	106,534	**18**	119,120	35	2,444	29,402
Total passenger delay	72,365	60	**82,176**	66	2,121	19,030
Passenger delay inequity	110,951	23	123,655	**26**	2,480	27,615
Total number of stops	107,356	298	124,503	328	**1,826**	16,725
Total pedestrian delay	106,792	285	123,278	313	2,142	**15,854**

Table 5: Range in single-objective optimized objective values (protected LT)

	Total vehicle delay (veh-sec)	Vehicle delay inequity (sec)	Total passenger delay (pass-sec)	Passenger delay inequity (sec)	Total number of stops (vehs)	Total pedestrian delay (ped-sec)
Value	38,631	280	42,327	302	654	13,548
Percent of minimum value	53%	1,556%	52%	1,162%	36%	85%

As with the green times, the objective values also had a wide range of values when only one objective was minimized. Several objectives had extremely large ranges. For example, the vehicle delay inequity ranged from 18 seconds to 298 seconds, a range of 280 seconds or over 1,500 percent of the minimized value. As with the single-objective optimized green times, the large range in values helps demonstrate the importance of MOO.

3.2.2 Permitted left turns

Table 6 and Table 7 below show the permitted LT green times when the objectives were optimized for one objective.

Table 6: Single-objective optimized green times (permitted LT)

Minimized objective	NS L/T/R green (sec)	EW L green (sec)	EW T/R green (sec)	Cycle length (sec)
Total vehicle delay	28.8	3.2	28.7	76.6
Vehicle delay inequity	35.9	11.4	32.1	95.4
Total passenger delay	28.8	3.2	28.7	76.6
Passenger delay inequity	35.9	11.4	32.1	95.4
Total number of stops	47.9	3.3	60.0	127.2
Total pedestrian delay	21.5	2.0	17.8	57.3

Table 7: Range in single-objective optimized green times (permitted LT)

NS L/T/R range (sec)	EW L range (sec)	EW T/R range (sec)	Cycle length (sec)
26.4	9.4	42.2	69.9

As with the protected LT, a large range in green times is present. The need to consider multiple objectives in the optimization is also required for this intersection for the

same reasons as with the protected LT. Variation in the NS approaches is present because all movements require a green time greater than the minimum, which provides a large range similar to the other green times. The ranges are larger for the permitted LT intersection, which indicates an even greater need for MOO. These trends are also observed in the objective values and their ranges, shown in Table 8 and Table 9.

Table 8: Single-objective optimized objective values (permitted LT)

Minimized Objective	Objective Value					
	Total vehicle delay (veh-sec)	**Vehicle delay inequity (sec)**	**Total passenger delay (pass-sec)**	**Passenger delay inequity (sec)**	**Total number of stops (vehs)**	**Total pedestrian delay (ped-sec)**
Total vehicle delay	**69,460**	59	77,460	65	2,253	17,634
Vehicle delay inequity	96,827	**20**	107,862	22	2,369	25,392
Total passenger delay	69,460	59	**77,460**	65	2,253	17,634
Passenger delay inequity	96,827	20	107,862	**22**	2,369	25,392
Total number of stops	96,843	286	108,396	315	**1,992**	23,300
Total pedestrian delay	99,050	83	109,707	92	2,420	**14,989**

Table 9: Range in single-objective optimized objective values (permitted LT)

	Total vehicle delay (veh-sec)	**Vehicle delay inequity (sec)**	**Total passenger delay (pass-sec)**	**Passenger delay inequity (sec)**	**Total number of stops (vehs)**	**Total pedestrian delay (ped-sec)**
Value	29,590	266	32,247	292	428	10,403
Percent of minimum value	43%	1,330%	42%	1,327%	21%	69%

The range in single-objective optimized objective values were also large for the permitted LT results, with the inequity objectives again exhibiting a range over 1,000 percent of the minimized objective value.

Both types of left turn treatments demonstrated the need for implementing MOO at the example intersection. The green times and objective values for each approach widely varied, suggesting the need for a balance between all objectives. The proposed MOO ranking methods introduced in Section 2.4 can determine solutions that provide this balance. These results are presented in the following section.

3.3 Multi-objective Optimization Results

This section presents the MOO results for both types of left turn treatments. In Sections 3.3.1 and 3.3.2, the tradeoff indices and mosaic plots are shown, followed by the top-ranked solutions provided by the ranking method, and concluding with analyses to determine the final solutions' sensitivity to objective removal.

3.3.1 Protected left turns

3.3.1.1 Tradeoff indices and mosaic plots

Figure 6 below shows the mosaic plot for the protected LT intersection. The tradeoff indices for each objective pair are labelled.

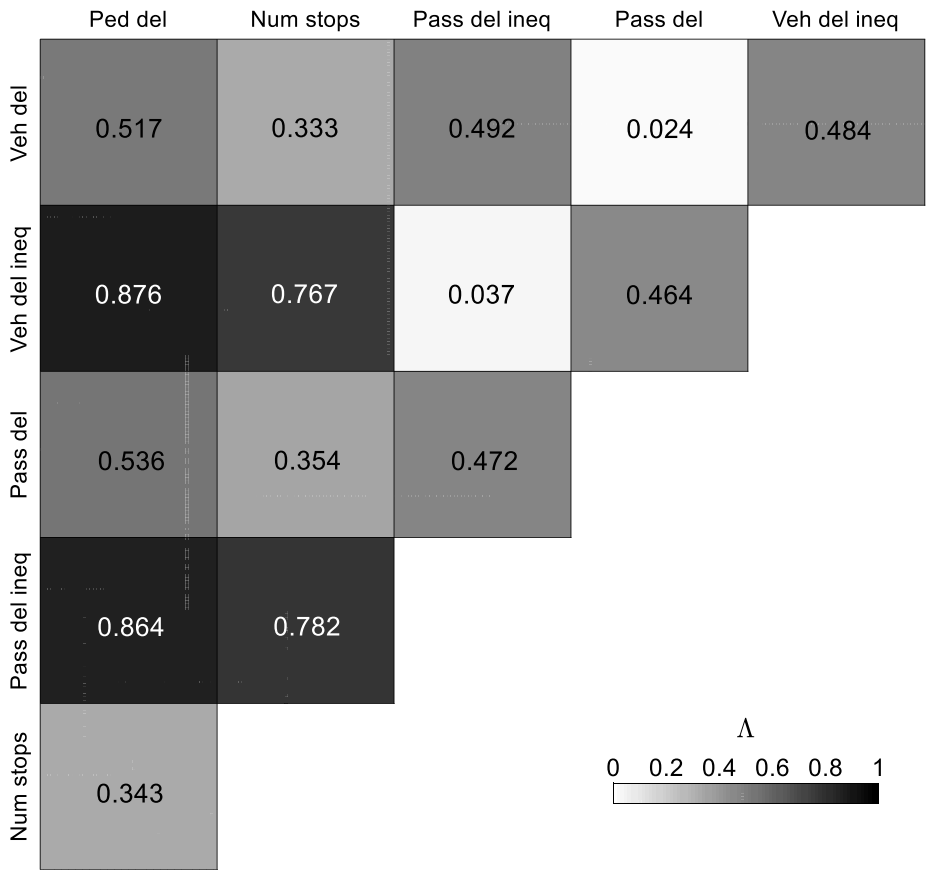

Figure 6: Homogenized mosaic plot (protected LT, first iteration)

There were several trends evident in the above mosaic plot. As described in Section 2.2, objective pairs with darker-colored squares (or higher tradeoff indices) exhibit more tradeoff. One trend that was expected was the fairly low tradeoff between the number of stops and both vehicle delay and passenger delay. This was expected because delays increase as the number of stops increase. Another expected trend was the low tradeoff between vehicle delay and passenger delay. The passenger delay is the vehicle delay weighted by the average occupancy, so the two objectives were expected to behave similarly when the passenger occupancies for each approach are similar (as is the case here). This is also true for the vehicle delay inequity and passenger delay inequity.

An unexpected tradeoff was the low tradeoff between pedestrian delay and number of stops. It was expected that there would be high tradeoff between the two: as the number of stops increases, the pedestrian delay should decrease because pedestrians can walk when vehicles are stopped. However, the opposite is true; as the number of stops decrease, the pedestrian delay also decreases. A possible explanation for this is because the NS pedestrian volumes are much heavier than the EW pedestrian volumes. Because the NS vehicle approaches are the minor approaches, they receive less green time and therefore experience a greater number of stops. The heavy NS pedestrian volumes therefore experience increased delay because of the short NS vehicle green times.

Another noticeable trend was the high tradeoff between the pedestrian delay and number of stops with the inequities. The inequity of the intersection increases as the pedestrian delay and number of stops decrease. The vehicle delay and passenger delay have the lowest average tradeoff with all other objectives, as shown in Table 10. Table 11 shows the similarities between the vehicle delay and passenger delay.

Table 10: Average homogenized tradeoff indices (protected LT, first iteration)

Total vehicle delay	Vehicle delay inequity	Total passenger delay	Passenger delay inequity	Total number of stops	Total pedestrian delay
0.370	0.526	0.370	0.530	0.516	0.627

Table 11: Total vehicle delay versus total passenger delay tradeoff indices (protected LT, first iteration)

Objective	Total vehicle delay	Total passenger delay	Absolute difference
Vehicle delay inequity	0.484	0.464	0.020
Passenger delay inequity	0.492	0.472	0.020
Total number of stops	0.333	0.354	0.021
Total pedestrian delay	0.517	0.536	0.020

After examining each objective's average homogenized tradeoff index, the passenger delay was deemed redundant because it had the lowest index and had very similar tradeoff indices with the vehicle delay as shown in Table 11. Because vehicle delay is the traditional objective used to time traffic signals, it was kept and the passenger delay objective was removed for the second MOO iteration. The mosaic plot for the second iteration is shown in Figure 7.

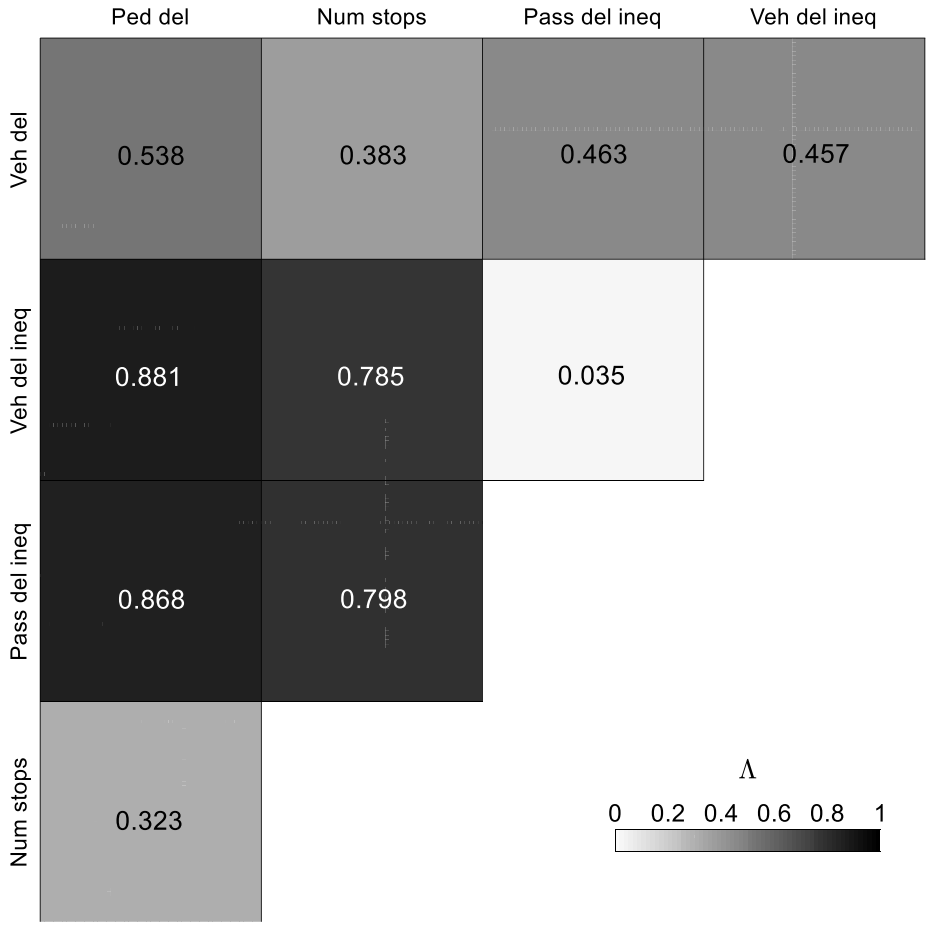

Figure 7: Homogenized mosaic plot (protected LT, second iteration)

The second iteration mosaic plot was relatively similar to the first iteration, with some small changes in tradeoff indices. The average homogenized tradeoff indices shown

in Table 12 also experienced relatively small changes. Removing the objective competing with vehicle delay increased the vehicle delay's tradeoff. The vehicle delay inequity and passenger delay inequity again exhibit the lowest tradeoff between two objectives. These objectives are not the least conflicting with other objectives, as shown in Table 12, but behave very similarly to each other as shown in Table 13.

Table 12: Average homogenized tradeoff indices (protected LT, second iteration)

Total vehicle delay	Vehicle delay inequity	Passenger delay inequity	Total number of stops	Total pedestrian delay
0.460	0.540	0.541	0.572	0.653

Table 13: Vehicle delay inequity versus passenger delay inequity tradeoff indices (protected LT, second iteration)

Objective	Vehicle delay inequity	Passenger delay inequity	Absolute difference
Total vehicle delay	0.457	0.463	0.005
Total number of stops	0.785	0.798	0.013
Total pedestrian delay	0.881	0.868	0.014

In the second iteration, the vehicle delay had the lowest homogenized tradeoff index. However, this objective was of high interest. Furthermore, as shown above in Table 13, the passenger delay inequity was found to be very similar to the vehicle delay inequity. Therefore, the passenger delay inequity objective was removed for the third MOO iteration. This was an example where a practitioner would not necessarily remove the objective with the lowest average homogenized tradeoff index, but instead remove an objective (passenger delay inequity) that has very similar tradeoffs with remaining objectives as another objective (vehicle delay inequity). The homogenized mosaic plot of the third iteration is shown in Figure 8.

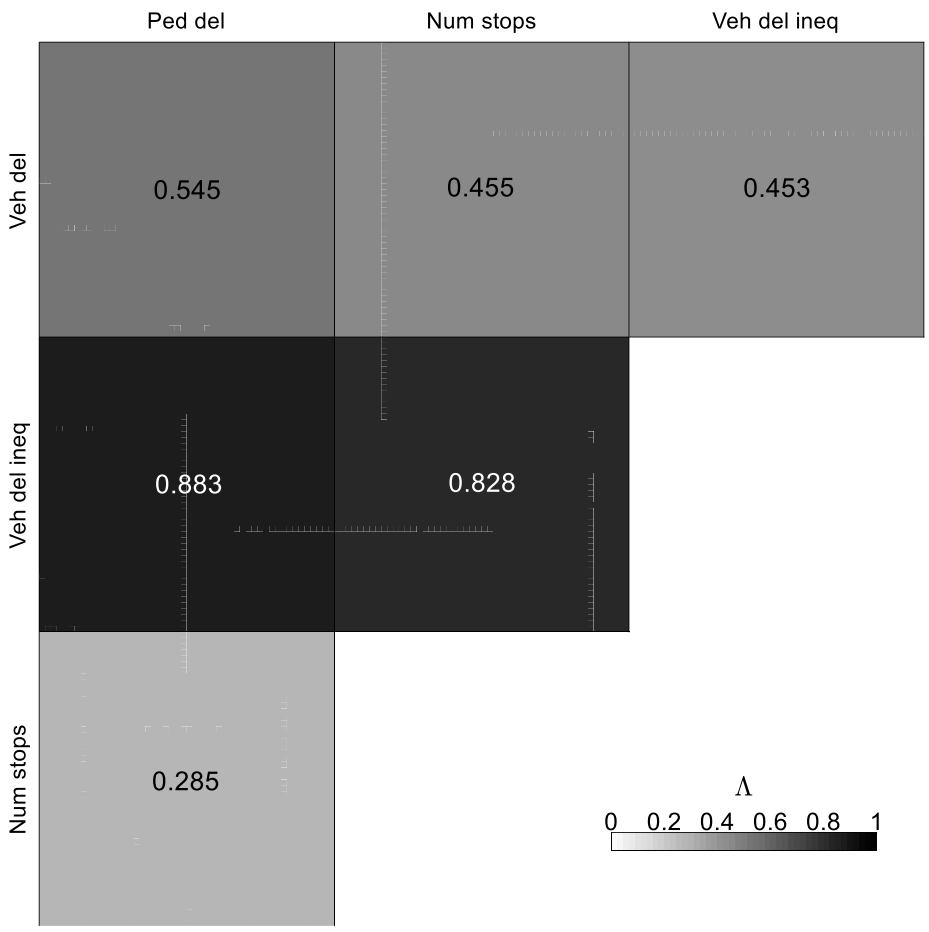

Figure 8: Homogenized mosaic plot (protected LT, third iteration)

The vehicle delay inequity exhibited the highest tradeoff with the pedestrian delay and number of stops. Pedestrian delay and number of stops exhibited the lowest tradeoff, and the remaining objective pairs exhibited average tradeoffs. The tradeoff indices remained relatively similar to those in the second iteration. Although the vehicle delay, number of stops, and pedestrian delay all exhibit low average homogenized tradeoff indices as shown in Table 14, they are objectives of interest so none were removed for a fourth iteration. It is noted that this decision is based on the opinion and methodology of the

decision-maker. Furthermore, the comparisons between pedestrian delay and number of stops, the least conflicting objectives, are provided below in Table 15.

Table 14: Average homogenized tradeoff indices (protected LT, third iteration)

Total vehicle delay	Vehicle delay inequity	Total number of stops	Total pedestrian delay
0.484	0.722	0.523	0.571

Table 15: Total pedestrian delay versus total pedestrian delay tradeoff indices (protected LT, third iteration)

Objective	Total number of stops	Total pedestrian delay	Absolute difference
Total vehicle delay	0.455	0.545	0.089
Vehicle delay inequity	0.828	0.883	0.055

Because the difference between the tradeoffs for these two objectives was relatively large and all remaining objectives were of high interest, this was the final iteration. From the first iteration to the third iteration, the objectives similar to removed redundant objectives experienced an increase in the average homogenized tradeoff indices. Meanwhile, the other objectives experienced a decrease. Removing one of the objectives of a non-competing pair will increase the overall tradeoff of the remaining objective. The overall tradeoffs of the other objectives will decrease because there is one less competing objective.

3.3.1.2 Ranking method results

The MOO results of each ranking method are shown in Table 16 (the green times) and Table 17 (the objective values). In Method 2, the vehicle delay was constrained to be no more than 20 percent greater than the minimum vehicle delay obtained in the single-objective optimization. In addition to the two methods, two different weighting factors were applied: one where all objectives were weighted equally, and one where the number

of stops and pedestrian delay were each weighted by a factor of 3.0. The number of stops was weighted because it has safety, environmental, and economical implications. A higher number of stops can increase rear-end collisions, increase emissions related to idling and accelerating, and cause brake wear and longitudinal grooving in pavement. The pedestrian delay was weighted because it is the only objective not specific to vehicles. These constraints and weighting factors were used for both left turn treatments. The objective values for removed objectives in the second and third iterations were manually calculated using the same formulas used in the MATLAB script.

Table 16: Multi-objective optimized green times (protected LT)

Method and weighting factors used	NS L green (sec)	NS T/R green (sec)	EW L green (sec)	EW T/R green (sec)	Cycle length (sec)
Iteration 1					
Method 1 – equal w_k	12.4	19.1	6.2	27.5	81.2
Method 1 – weighted w_k	11.5	19.1	6.0	30.9	83.5
Method 2 – equal w_k	12.9	19.1	7.1	30.3	85.4
Method 2 – weighted w_k	10.4	19.1	5.3	26.7	77.5
Iteration 2					
Method 1 – equal w_k	13.8	19.1	8.0	28.2	85.1
Method 1 – weighted w_k	10.7	19.1	5.3	28.4	79.5
Method 2 – equal w_k	12.0	19.1	6.6	28.7	82.4
Method 2 – weighted w_k	10.7	19.1	5.6	26.9	78.3
Iteration 3					
Method 1 – equal w_k	12.2	19.1	6.9	28.3	82.5
Method 1 – weighted w_k	10.6	19.1	4.9	40.6	91.2
Method 2 – equal w_k	11.8	19.1	6.4	28.5	81.8
Method 2 – weighted w_k	10.4	19.1	4.8	40.0	90.3

Table 17: Multi-objective optimized objective values (protected LT)

Method and weighting factors used	Objective Value					
	Total vehicle delay (veh-sec)	Vehicle delay inequity (sec)	Total passenger delay (pass-sec)	Passenger delay inequity (sec)	Total number of stops (vehs)	Total pedestrian delay (ped-sec)
Iteration 1						
Method 1 – equal w_k	90,296	23	101,169	37	2,442	22,400
Method 1 – weighted w_k	80,597	27	90,712	45	2,358	21,314
Method 2 – equal w_k	86,601	23	97,195	40	2,400	22,915
Method 2 – weighted w_k	85,492	26	96,027	43	2,429	20,771
Iteration 2						
Method 1 – equal w_k	97,916	20	109,548	35	2,462	24,274
Method 1 – weighted w_k	81,725	28	92,118	44	2,392	20,695
Method 2 – equal w_k	86,768	24	97,581	40	2,416	22,235
Method 2 – weighted w_k	86,424	25	96,960	42	2,431	21,119
Iteration 3						
Method 1 – equal w_k	89,318	23	100,211	39	2,431	22,623
Method 1 – weighted w_k	72,927	45	82,876	66	2,150	19,349
Method 2 – equal w_k	86,542	24	97,083	40	2,417	22,048
Method 2 – weighted w_k	72,922	45	82,865	67	2,157	19,245

The first two iterations are shown for completion; the discussion will focus on the third iteration because its results are the final results used. The equal w_k results for Methods 1 and 2 are very similar as each approach's green times did not greatly vary. The NS T/R green was the only green time that all ranking methods selected the same best green time. As mentioned in Section 3.2.1, this is likely because the minimum green time was more than enough for the low NS vehicle volumes. Likewise, the objective values were relatively

similar. Although some differences seem large, such as the 2,776 vehicle-seconds of total vehicle delay, it equates to approximately one second per vehicle. The weighted w_k results for Methods 1 and 2 exhibited the same pattern.

An additional trend to note for these results are the lower objective values for the weighted objectives. The number of stops and pedestrian delay values are noticeably lower for the weighted results compared to the equally-weighted results, regardless of the method used. Also, most approaches' green times were similar when comparing the weighted to equally-weighted results. The EW T/R green time, however, was approximately 12 seconds longer for weighted cases. This suggests a longer green time is needed to decrease number of stops and pedestrian delay.

Most optimized green times fell within the range of the single-objective optimized green times, with the exception of the EW T/R green times. While it was expected that all MOO green times would fall in the SOO green times, it is possible for this not to happen. The combined effect of all four green times influence the objective values. One MOO green time falling outside the SOO range is logical, particularly because it is relatively close to being within range. This demonstrates the ability of MOO to balance different objectives.

3.3.1.3 Sensitivity analysis

The removal of redundant objectives one at a time raises the concern of how the final ranked solutions would change if different redundant objectives were removed (e.g. vehicle delay versus passenger delay) or if the objectives were removed in a different order (e.g. passenger delay first and passenger delay inequity second, or vice versa). In order to address this potential issue, a sensitivity analysis was conducted to determine the effect of

different objective removal strategies. Four cases were tested and are described below in Table 18.

Table 18: Sensitivity analysis test scenarios

Case	Iteration 1 removal	Iteration 2 removal
Case A	passenger delay	passenger delay inequity
Case B	vehicle delay	vehicle delay inequity
Case C	passenger delay	vehicle delay inequity
Case D	vehicle delay	passenger delay inequity

The results of the unweighted Method 1 solutions are shown in Table 19.

Table 19: Sensitivity analysis results (protected LT)

Case	NS L (sec)	NS T/R (sec)	EW L (sec)	EW T/R (sec)	Cycle length (sec)
Case A	12.1	19.1	6.6	30.2	84.0
Case B	13.4	19.1	5.0	29.4	82.9
Case C	13.4	19.1	5.0	29.4	82.9
Case D	12.2	19.1	6.7	29.2	83.2
Range	**1.36**	**0.00**	**1.70**	**1.02**	**1.09**

The ranges of green times are relatively small. This indicates the objective removal order does not affect the final solutions because all green times are very similar, regardless of which case was tested. The NS T/R was exactly the same regardless of the objective removal order. These results suggest the final solution is not sensitive to the objective removal process.

3.3.2 Permitted left turns

3.3.2.1 Tradeoff indices and mosaic plots

The mosaic plot for the first iteration of the permitted LT intersection is shown below with each objective pair's tradeoff indices.

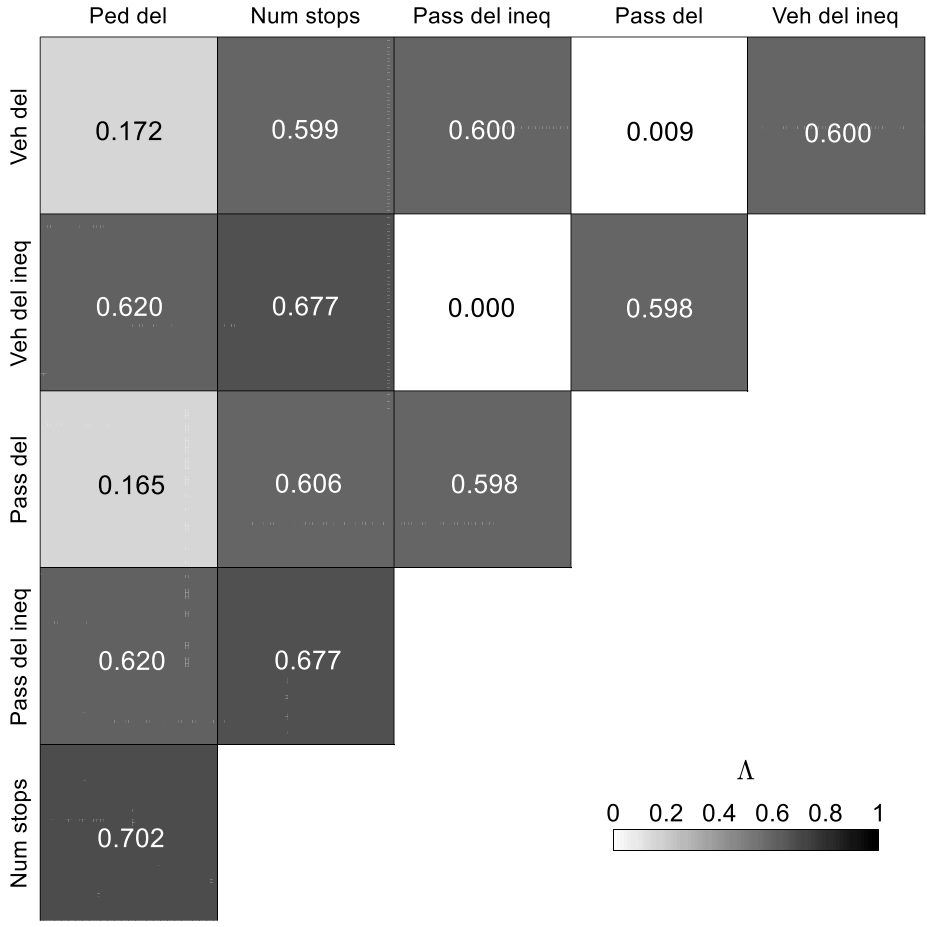

Figure 9: Homogenized mosaic plot (permitted LT, first iteration)

Overall, the permitted LT mosaic plot shows less tradeoff than the protected LT mosaic plot. The two mosaic plots look relatively similar with some noticeable exceptions. The tradeoffs between pedestrian delay and both vehicle and passenger delays increased. This is likely because left-turning vehicles must yield to pedestrians because there is no

protected left-turning phase where pedestrians do not receive the "WALK" indication. Because these vehicles must yield, the vehicle and passenger delays increase. Another difference is that the tradeoffs between number of stops and all three delays (vehicle, passenger, and pedestrian) all decreased.

The average homogenized tradeoff indices, shown in Table 20, were also similar to the LT protected indices with two noticeable exceptions. The number of stops decreased and the pedestrian delay increased. This is consistent with the changes in the tradeoff indices discussed earlier. The vehicle delay and passenger delay both have similar average homogenized tradeoff indices, as do the vehicle delay inequity and passenger delay inequity. The vehicle delay and passenger delay have the lowest values and were compared to determine their tradeoff similarities with other objectives. These results are shown in Table 21.

Table 20: Average homogenized tradeoff indices (permitted LT, first iteration)

Total vehicle delay	Vehicle delay inequity	Total passenger delay	Passenger delay inequity	Total number of stops	Total pedestrian delay
0.396	0.499	0.395	0.499	0.652	0.456

Table 21: Total vehicle delay versus total passenger delay tradeoff indices (permitted LT, first iteration)

Objective	Total vehicle delay	Total passenger delay	Absolute difference
Vehicle delay inequity	0.600	0.598	0.002
Passenger delay inequity	0.600	0.598	0.002
Number of stops	0.599	0.606	0.008
Total pedestrian delay	0.172	0.165	0.007

As with the protected LT intersection, the passenger delay was removed for the second iteration because of its low average homogenized tradeoff index and its similarity

to the more conventional vehicle delay. The second iteration mosaic plot is shown in Figure 10.

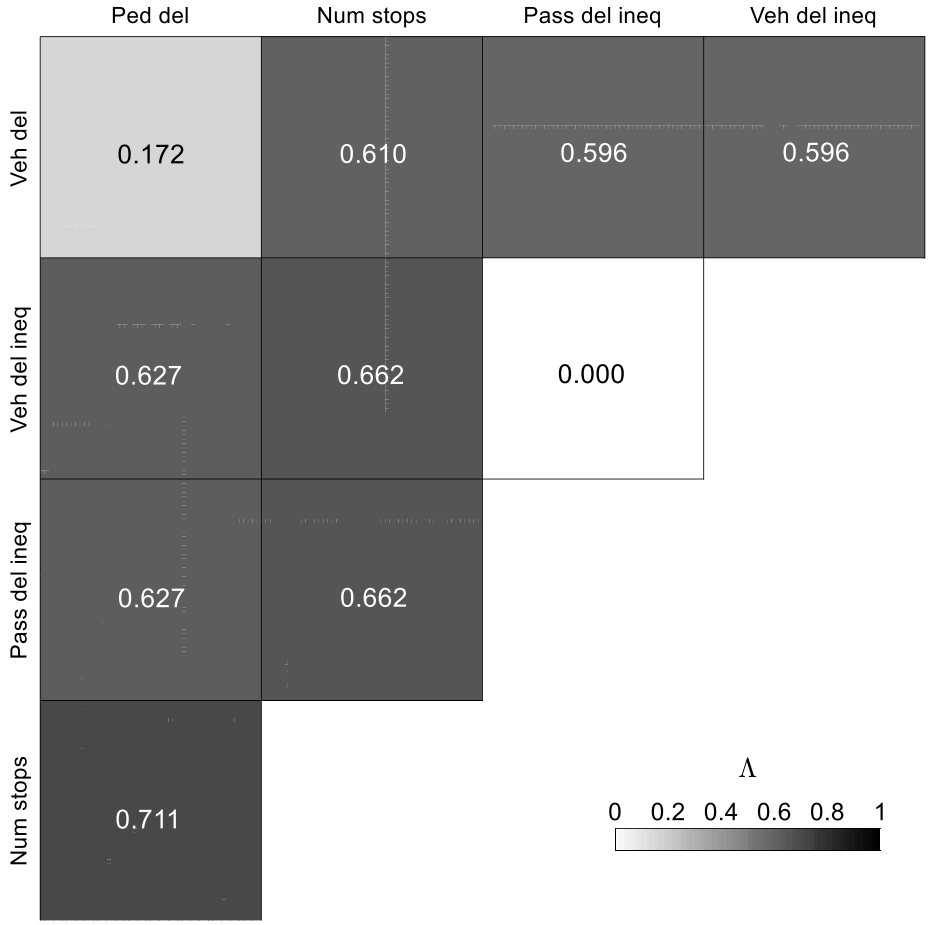

Figure 10: Homogenized mosaic plot (permitted LT, second iteration)

After removing the passenger delay, the same LT protected differences as the first iteration were observed. The tradeoff between pedestrian delay and vehicle delay increased, and the tradeoffs between number of stops and the remaining delays (vehicle and pedestrian) decreased.

As with the protected LT case, the vehicle delay inequity and passenger delay inequity were investigated for redundancy because they have the same (lowest) average

homogenized tradeoff index, as shown in Table 22. The differences between these objectives' tradeoffs are shown in Table 23.

Table 22: Average homogenized tradeoff indices (permitted LT, second iteration)

Total vehicle delay	Vehicle delay inequity	Passenger delay inequity	Total number of stops	Total pedestrian delay
0.493	0.471	0.471	0.661	0.534

Table 23: Vehicle delay inequity versus passenger delay inequity tradeoff indices (permitted LT, second iteration)

Objective	Vehicle delay inequity	Passenger delay inequity	Absolute difference
Vehicle delay	0.596	0.596	0.000
Number of stops	0.662	0.662	0.000
Total pedestrian delay	0.627	0.627	0.000

As with the protected LT, the passenger delay inequity was removed for the third iteration because of its similarity to vehicle delay inequity. The two objectives had the same tradeoff with every other objective, showing the two objectives exhibited very high redundancy. The third iteration mosaic plot with tradeoff indices is shown below in Figure 11.

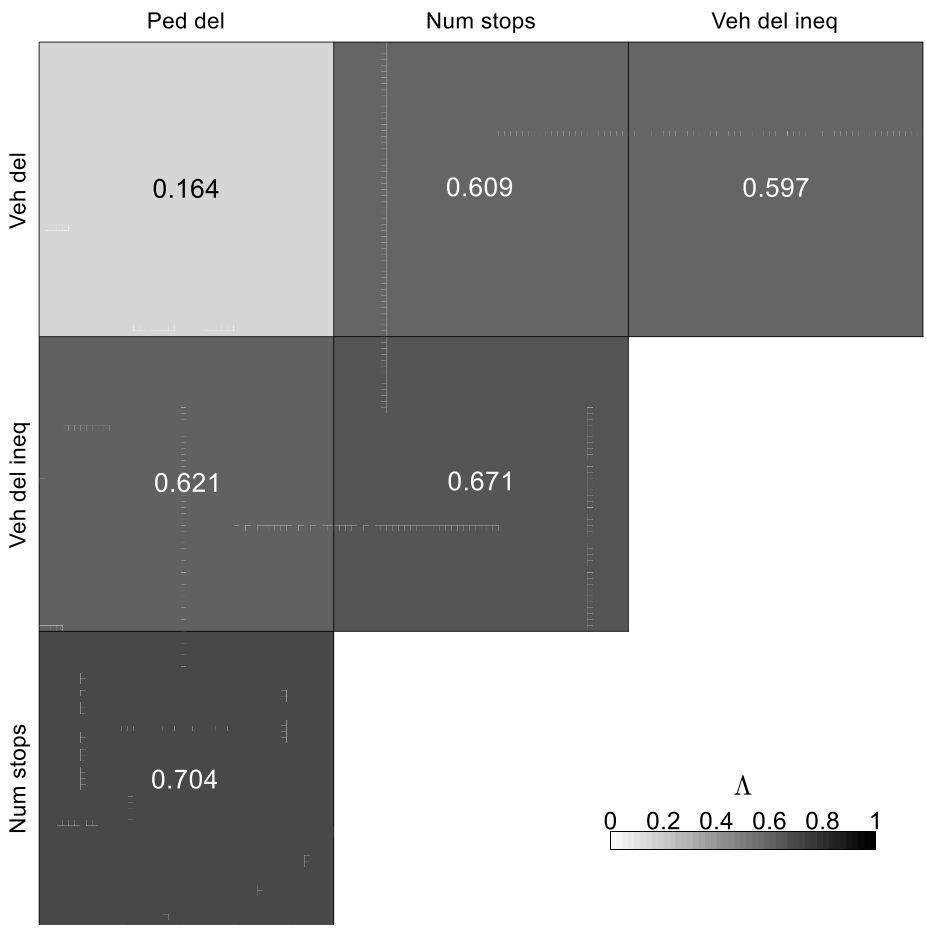

Figure 11: Homogenized mosaic plot (permitted LT, third iteration)

The same differences between the protected LT mosaic plots from the first two iterations were also seen in the third iteration. The pedestrian and vehicle delay tradeoff decreased and the number of stops and pedestrian delay tradeoff increased.

Most objective pairs have a tradeoff greater than 0.500, meaning that over 50 percent of solutions exhibit tradeoff between the two objectives. Pedestrian delay and vehicle delay had a low tradeoff. Although unexpected, this can likely be explained by the same reason pedestrian delay and number of stops had a low tradeoff (in Section 3.3.1.1).

The pedestrian-heavy direction is NS, while the vehicle-heavy direction is EW. If the NS approaches get more green time, the many pedestrians experience less delay while the few vehicles experience more delay. If the EW approaches get more green time, the many vehicles experience less delay while the few pedestrians experience more delay.

The average homogenized tradeoff indices shown in Table 24 were deemed acceptable for the final iteration.

Table 24: Average homogenized tradeoff indices (permitted LT, third iteration)

Total vehicle delay	Vehicle delay inequity	Total number of stops	Total pedestrian delay
0.457	0.630	0.661	0.496

As with the protected LT intersection, the vehicle delay and vehicle delay inequity average homogenized tradeoff indices increased from the first to third iteration because their corresponding redundant objectives were removed. The number of stops and pedestrian delay indices were relatively constant, increasing by 0.009 and 0.040 respectively.

3.3.2.2 Ranking method results

The green times and objective values are shown below in Table 25 and Table 26.

Table 25: Multi-objective optimized green times (permitted LT)

Method and weighting factors used	NS L/T/R green (sec)	EW L green (sec)	EW L green (sec)	Cycle length (sec)
Iteration 1				
Method 1 – equal w_k	28.7	6.0	25.6	76.3
Method 1 – weighted w_k	28.2	5.3	25.4	74.9
Method 2 – equal w_k	29.2	6.4	26.0	77.6
Method 2 – weighted w_k	28.0	5.7	24.8	74.5
Iteration 2				
Method 1 – equal w_k	29.3	6.7	25.8	77.8
Method 1 – weighted w_k	26.8	5.1	23.1	71.0
Method 2 – equal w_k	29.1	6.3	25.9	77.3
Method 2 – weighted w_k	27.5	5.3	24.2	73.0
Iteration 3				
Method 1 – equal w_k	28.5	6.0	25.2	75.7
Method 1 – weighted w_k	25.2	4.0	21.9	67.1
Method 2 – equal w_k	28.8	6.2	25.5	76.5
Method 2 – weighted w_k	26.1	4.6	22.8	69.5

Table 26: Multi-objective optimized objective values (permitted LT)

Method and weighting factors used	Objective Value					
	Total vehicle delay (veh-sec)	**Vehicle delay inequity (sec)**	**Total passenger delay (pass-sec)**	**Passenger delay inequity (sec)**	**Total number of stops (vehs)**	**Total pedestrian delay (ped-sec)**
Iteration 1						
Method 1 – equal w_k	82,022	23	91,274	26	2,361	19,658
Method 1 – weighted w_k	79,122	25	88,059	28	2,351	19,037
Method 2 – equal w_k	83,176	23	92,562	25	2,363	20,033
Method 2 – weighted w_k	82,047	24	91,272	26	2,367	19,219
Iteration 2						
Method 1 – equal w_k	85,363	22	95,338	24	2,372	20,293
Method 1 – weighted w_k	85,047	24	94,796	26	2,385	18,567
Method 2 – equal w_k	83,016	23	92,440	25	2,363	19,941
Method 2 – weighted w_k	82,188	24	91,304	27	2,370	18,890
Iteration 3						
Method 1 – equal w_k	83,091	23	92,577	25	2,368	19,565
Method 1 – weighted w_k	81,906	29	90,752	32	2,383	17,338
Method 2 – equal w_k	83,153	23	92,948	25	2,366	19,791
Method 2 – weighted w_k	82,242	26	91,167	28	2,380	17,971

Trends from the protected LT case were also noticed in the permitted LT third iteration. The equally-weighted solutions resulted in very similar results as each other, as did the weighted solutions. When comparing the unconstrained delay solutions (Method 1) to the constrained delay solutions (Method 2), the constrained solutions actually had a higher vehicle delay. While this was unexpected, the delay was still within 120 percent of the single-objective optimized delay value. The weighted solutions did not always provide

a lower objective value for both weighted objectives. In some cases, the weighted number of stops would be higher than the unweighted number of stops, but the weighted pedestrian delay was still lower than the unweighted pedestrian delay. Because these objectives had a high tradeoff (0.704), it would be difficult to lower both. At least one weighted objective value was always lower than its corresponding unweighted objective value.

The NS L/T/R green times were close to the sum of the NS L and NS T/R green times in the protected case, as shown below in Table 27.

Table 27: Sum of protected NS L and NS T/R green times versus permitted NS L/T/R green times

Method and weight	NS L + NS T/R (sec)	NS L/T/R (sec)
Method 1 – equal w_k	31.3	28.5
Method 1 – weighted w_k	29.7	25.2
Method 2 – equal w_k	30.9	28.8
Method 2 – weighted w_k	29.5	26.1

3.3.2.3 Sensitivity analysis

As with the protected LT intersection, a sensitivity analysis was performed on the permitted LT intersection using the same cases in Table 18. The results of the unweighted Method 1 solutions are shown in Table 28.

Table 28: Sensitivity analysis results (permitted LT)

Case	NS L (sec)	EW L (sec)	EW T/R (sec)	Cycle length (sec)
Case A	27.7	5.8	24.2	73.7
Case B	28.0	5.9	24.5	74.4
Case C	27.6	5.6	24.2	73.4
Case D	28.1	5.8	24.7	74.6
Range	**0.47**	**0.32**	**0.49**	**1.19**

The ranges between different cases are even smaller than the protected LT intersection, with each green time varying by less than one second. This again suggests the objectives are not sensitive to the redundant objective removal process.

3.3.3 Multi-objective optimization summary

Two intersections were tested: one with protected NS left turns and one with permitted NS left turns. There were similarities and differences between these cases.

Both intersections had a relatively similar mosaic plots for each iteration, though some objective pairs exhibited noticeably different tradeoffs between the two intersections. This suggests the tradeoff between most objectives is independent of the left-turning treatment. Both cases demonstrated the validity of the weighting factor and Method 2 constraint. Also, both cases had the same objectives removed due to redundancy. After the first iteration, the passenger delay was removed because it had a low average homogenized tradeoff index and was very similar to the vehicle delay. After the second iteration, the passenger delay inequity was removed because it was very similar to the vehicle delay inequity. In the LT protected intersection, this was an example where a high-tradeoff objective was removed from the iteration because it was too similar to another objective. This demonstrates the importance of considering both methods described in Section 2.3 for redundant objective removal. In the sensitivity analyses, both intersections showed the final solutions are independent of the redundant objective removed or the removal order.

After the third iteration, the objectives in all four cases were deemed to display enough tradeoff and no more objectives were removed. This action is dependent on the opinion of the decision-maker; e.g. if another decision-maker was solving this problem,

they may decide to continue onto a fourth iteration. Ranking methods are applied to the final MOO iteration, although here they were also applied to the first and second iterations to show the evolution of the solutions. A decision-maker would use the solution produced by their desired ranking method, or the one of four that matches their desired weighting factor and constraint.

The MOO results for the two intersections were shown separately for the sake of discussion. In order to compare both intersection results, all eight top-ranked solutions for both intersections are shown in Table 29 in the ratio products' ascending order.

Table 29: Comparison of protected and permitted LT top-ranked results

LT treatment, ranking method, w_k	Ratio product	NS L/T/R (permitted) or NS L and NS T/R (protected) (sec)		EW L (sec)	EW T/R (sec)	Cycle length (sec)
Permitted, Method 2, unweighted	1.52	28.8	-	6.2	25.5	76.5
Protected, Method 2, unweighted	1.80	11.8	19.1	6.4	28.5	81.8
Permitted, Method 1, unweighted	2.14	28.5	-	6.0	25.2	75.6
Protected, Method 1, unweighted	2.93	12.2	19.1	6.9	28.3	82.6
Permitted, Method 2, weighted	3.03	26.1	-	4.6	22.8	69.4
Permitted, Method 1, weighted	4.53	25.2	-	4.0	21.9	67.1
Protected, Method 2, weighted	4.96	10.4	19.1	4.8	40.0	90.3
Protected, Method 1, weighted	7.43	10.6	19.1	4.9	40.6	91.2

The weighted solutions logically had the highest ratio products because the objective value ratios were increased. Constraining the vehicle delay (e.g. the Method 2 solutions) provides lower ratio products. The ratio products of the Method 2 solutions were both lower than the Method 1 solutions for unweighted solutions. For weighted solutions, a Method 2 solution provided the lowest ratio product. This is likely because the vehicle delay objective value ratio was excluded from the ratio product calculation. Interestingly, the permitted Method 1 solution had a lower ratio product than the protected Method 2

solution—despite including the vehicle delay objective value ratio in the ratio product calculation.

The permitted LT treatments provide lower ratio products than protected LT treatments. For unweighted solutions, the permitted solution did better than the protected solution for the same vehicle delay constraint (e.g. Method 1 and Method 2). For weighted solutions, both permitted solutions had lower ratio products than the protected solutions. These results demonstrate that not only can the ranking methodology be used to determine signal timings, but also the LT treatment. If a decision-maker was considering either protected or permitted left turns, the results here would suggest using permitted left turns. It is noted that these results are dependent on the example problem. A different intersection geometry, vehicle and pedestrian volumes, or objectives would likely drastically change the results.

4.0 Conclusions and Future Work

Traffic signal timing optimization has been the subject of considerable research interest for over two decades, with the more recent work considering multiple objectives in the optimization process. Most MOO studies only used two or three objectives, which are not enough to fully capture the complexities of intersection operations. While the range of objectives considered in previous work has been diverse, the relationships cannot be observed if only one, two, or three objectives are used to optimize traffic signal timings.

Existing literature does not provide methods for a decision-maker to easily identify or quantify the tradeoff between objectives. Consequently, there is no way to quickly determine the conflict or degree of tradeoff between objectives. Without this knowledge, the objectives at an intersection cannot be fully understood. Existing work also lacks guidance for a decision-maker in selecting which MOO-generated optimal solution is the "best" solution for a particular scenario. While many papers have used MOO in signal timing optimization, none have proposed a methodology to apply one solution to an intersection—though some papers have highlighted this as a gap in knowledge. Without such a methodology, the usefulness of MOO is diminished as the decision-maker is required to select from many optimal solutions. There is also no guidance on the identification and removal process of redundant objectives. Removing redundant objectives decreases the problem dimensionality while ensuring the optimization includes only objectives that conflict with each other.

This work introduced the existing tradeoff index and mosaic plot to the traffic engineering research field. The tradeoff index identifies and quantifies the tradeoffs

between objectives, while the mosaic plot presents the tradeoffs in an easily understood graphic. Based on the tradeoff index, new indices were proposed for dimensionality reduction and ranking the optimal solutions. The average homogenized tradeoff index was used in one of the two proposed methods to remove redundant objectives. The objective value ratio and ratio product were used to rank the solutions resulting from the MOO. Four different ranking methods were proposed as four combinations of objective constraints and objective weighting factors. The ranking methodology is independent of the objective definition and optimization processes used.

A numerical example was used to demonstrate the proposed indices and methods in use, as well as demonstrating the validity of the methodology. Six diverse objectives were used, including ones that consider multimodal operations and the delay inequity within an intersection. Two different intersections were used, with the left turn treatments varying in each case. Solutions and their corresponding objective values of each iteration were shown and discussed. Finally, sensitivity analyses were performed to determine the effect of redundant objective removal on final solutions. It was found that the removal process did not noticeably affect the final solutions. Each intersection resulted in four "best" optimal solutions depending on the objective constraint and weighting factor, a significant decrease from the population size of 2,500. The decision-maker would use the solution that uses their desired objective constraint and weighting factor to implement at the intersection.

There are several possibilities to continue or add to this work:

- Define a process to select the weighting factors used. While they may be chosen somewhat arbitrarily, a decision-maker may desire a more methodological approach.
- Apply the process to a coordinated arterial with multiple signalized intersections. In addition to the objective tradeoffs within an intersection, the tradeoffs between intersections can be determined.
- Repeat the process with more realistic objective definitions. The objectives used here were defined analytically but could also be obtained through simulations. For example, the number of stops could be outputted from a simulation rather than estimated. Simulations could also obtain direct measures of safety or emissions, such as number of conflicts or emissions released, rather than surrogate measures.
- Investigate other methods to obtain the objective value ratio. The proposed method here divides a solution's objective value by the minimum objective value. However, a potential way to calculate the objective value ratio is to divide the solution's objective value by a threshold value. If a solution's quotient is less than or equal to one, meaning the value is acceptable, its objective value ratio is set to one. Otherwise, the value is set to the quotient. The effects of this calculation method on the ratio products could be determined in a future study.
- Consider the effects of a potential option for redundant objective removal. When one of two redundant objectives is removed, the remaining objective can be weighted such that it is twice as important. The optimization would

consider the effects of both objectives while still reducing the dimensionality of the problem. The results proposed here can be compared to the results proposed earlier in this paper.

A review of literature has determined there is much interest in multi-objective signal timing optimization. This work helps a decision-maker understand objective relationships at an intersection, reduces the dimensionality of the optimization problem, and presents a method to select the solution best-suited for a particular intersection.

References

1. Schrank., D., B. Eisele., T. Lomax., and J. Bak. *2015 Urban Mobility Scorecard*. College Station, TX, 2015.

2. Koonce, P., L. Rodegerdts, K. Lee, and S. Quayle. Traffic Signal Timing Manual. 2008, p. 273. https://doi.org/FHWA-HOP-08-024.

3. Garber, N. J., and L. A. Hoel. *Traffic and Highway Engineering*. Cengage Learning, Toronto, 2009.

4. Highway Capacity Manual (HCM). Transportation Research Board (TRB), 5th Edition. 2010.

5. Yang, Z., W. Wang, S. Chen, H. Ding, and X. Li. Genetic Algorithm for Multiple Bus Line Coordination on Urban Arterial. *Computational Intelligence and Neuroscience*, Vol. 2015, 2015. https://doi.org/10.1155/2015/868521.

6. Sun, D., R. F. Benekohal, and S. T. Waller. Multi-Objective Traffic Signal Timing Optimization Using Non-Dominated Sorting Genetic Algorithm. *Intelligent Vehicles Symposium, 2003. Proceedings. IEEE*, 2003, pp. 198–203. https://doi.org/10.1109/IVS.2003.1212908.

7. Girianna, M., and R. F. Benekohal. Using Genetic Algorithms to Design Signal Coordination for Oversaturated Networks. *Journal of Intelligent Transportation Systems*, Vol. 8, No. 2, 2004, pp. 117–129. https://doi.org/10.1080/15472450490435340.

8. Lertworawanich, P., M. Kuwahara, and M. Miska. A New Multiobjective Signal Optimization for Oversaturated Networks. *IEEE Transactions on Intelligent Transportation Systems*, Vol. 12, No. 4, 2011, pp. 967–976. https://doi.org/10.1109/TITS.2011.2125957.

9. Chen, X., D. Qian, and D. Shi. Multi-Objective Optimization Method of Signal Timing for the Non-Motorized Transport at Intersection. *Journal of Transportation Systems Engineering and Information Technology*, Vol. 11, No. 2, 2011, pp. 106–111. https://doi.org/http://dx.doi.org/10.1016/S1570-6672(10)60118-3.

10. Christofa, E., and A. Skabardonis. Traffic Signal Optimization with Application of Transit Signal Priority to an Isolated Intersection. *Transportation Research Record 2259*, 2011, pp. 192–201. https://doi.org/10.3141/2259-18.

11. Aziz, H. M. A., and S. V. Ukkusuri. Unified Framework for Dynamic Traffic Assignment and Signal Control with Cell Transmission Model. *Transportation Research Record 2311*, 2012, pp. 73–84.

12. Roshandeh, A. M., Z. Li, S. Zhang, H. S. Levinson, and X. Lu. Vehicle and Pedestrian Safety Impacts of Signal Timing Optimization in a Dense Urban Street Network. *Journal of Traffic and Transportation Engineering (English Edition)*, Vol. 3, No. 1, 2016, pp. 16–27. https://doi.org/10.1016/j.jtte.2016.01.001.

13. Zhang, L., W. Wu, and X. Huang. A Dynamic Optimization Model for Adjacent Signalized Intersection Control Systems Based on the Stratified Sequencing Method. *Journal of Highway and Transportation Research and Development*

(English Ed.), Vol. 10, No. 1, 2016, pp. 85–91.

14. Zhao, X., M. Feng, H. Li, and T. Zhang. Optimization of Signal Timing at Critical Intersections for Evacuation. *Procedia Engineering*, Vol. 137, 2016, pp. 334–342. https://doi.org/10.1016/j.proeng.2016.01.266.

15. Yu, C., W. Ma, K. Han, and X. Yang. Optimization of Vehicle and Pedestrian Signals at Isolated Intersections. *Transportation Research Part B: Methodological*, Vol. 98, 2017, pp. 135–153. https://doi.org/10.1016/j.trb.2016.12.015.

16. Wei, X., L. Cheng, and C. Sun. Optimization Research on Unsaturated Intersections Based on Traffic Delay. *CICTP 2016: Green and Multimodal Transportation and Logistics. Proceedings.*, 2016, pp. 1100–1109.

17. Noaeen, M., A. A. Rassafi, and B. H. Far. Traffic Signal Timing Optimization by Modelling the Lost Time Effect in the Shock Wave Delay Model. *International Conference on Transportation and Development 2016: Projects and Practices for Prosperity - Proceedings of the 2016 International Conference on Transportation and Development*, 2016, pp. 397–408. https://doi.org/10.1061/9780784479926.037.

18. Farnoush, K., and E. Christofa. Emission-Based Signal Timing Optimization for Isolated Intersections. *Transportation Research Record 2487*, 2015, pp. 1–14. https://doi.org/10.3141/2487-01.

19. Wong, C. K., and S. C. Wong. Lane-Based Optimization of Signal Timings for Isolated Junctions. *Transportation Research Part B: Methodological*, Vol. 37, 2003, pp. 63–84. https://doi.org/10.1016/S0191-2615(01)00045-5.

20. Schmöcker, J.-D., S. Ahuja, and M. G. H. Bell. Multi-Objective Signal Control of Urban Junctions - Framework and a London Case Study. *Transportation Research Part C: Emerging Technologies*, Vol. 16, No. 4, 2008, pp. 454–470. https://doi.org/10.1016/j.trc.2007.09.004.

21. Yin, Y. Multiobjective Bilevel Optimization for Transportation Planning and Management Problems. *Journal of Advanced Transportation*, Vol. 36, No. 1, 2002, pp. 93–105. https://doi.org/10.1002/atr.5670360106.

22. Abu-Lebdeh, G., and R. F. Benekohal. Development of Traffic Control and Queue Management Procedures for Oversaturated Arterials. *Transportation Research Record 1603*, 1997, pp. 119–127.

23. Abbas, M. M., and A. Sharma. Multiobjective Plan Selection Optimization for Traffic Responsive Control. *Journal of Transportation Engineering*, Vol. 132, No. 5, 2006, pp. 376–384. https://doi.org/10.1061/(ASCE)0733-947X(2006)132:5(376).

24. Kesur, K. B. Generating More Equitable Traffic Signal Timing Plans. *Transportation Research Record: Journal of the Transportation Research Board*, Vol. 2192, No. 1, 2011, pp. 108–115. https://doi.org/10.3141/2192-10.

25. Zhang, L., Y. Yin, and S. Chen. Robust Signal Timing Optimization with Environmental Concerns. *Transportation Research Part C: Emerging Technologies*, Vol. 29, 2013, pp. 55–71. https://doi.org/10.1016/j.trc.2013.01.003.

26. Stevanovic, A., J. Stevanovic, and C. Kergaye. Optimizing Signal Timings To Improve Safety of Signalized Arterials. *Third International Conference on Road*

Safety and Simulation. Proceedings., 2011.

27. Stevanovic, A., J. Stevanovic, J. So, and M. Ostojic. Multi-Criteria Optimization of Traffic Signals: Mobility, Safety, and Environment. *Transportation Research Part C: Emerging Technologies*, Vol. 55, 2015, pp. 46–68. https://doi.org/http://dx.doi.org/10.1016/j.trc.2015.03.013.

28. Branke, J., P. Goldate, and H. Prothmann. Actuated Traffic Signal Optimization Using Evolutionary Algorithms. *The 6th European Congress and Exhibition on Intelligent Transport Systems and Services*. http://citeseerx.ist.psu.edu/viewdoc/summary?doi=10.1.1.128.8683.

29. Yun, I., and B. Park. *Stochastic Optimization Method for Coordinated Actuated Signal Systems*. Charlottesville, VA, 2005.

30. Park, B., C. Messer, and T. Urbanik. Traffic Signal Optimization Program for Oversaturated Conditions: Genetic Algorithm Approach. *Transportation Research Record*, Vol. 1683, No. 1, 1999, pp. 133–142. https://doi.org/10.3141/1683-17.

31. Hadi, M. A., and C. E. Wallace. Hybrid Genetic Algorithm to Optimize Signal Phasing and Timing. *Transportation Research Record 1421*, 1993, pp. 104–112.

32. Foy, M. D., R. F. Benekohal, and D. E. Goldberg. Signal Timing Determination Using Genetic Algorithms. *Transportation Research Record 1365*, 1992, pp. 108–115.

33. Park, B., C. J. Messer, and T. Urbanik II. Enhanced Genetic Algorithm for Signal-Timing Optimization of Oversaturated Intersections. *Transportation Research*

Record 1727, 2000, pp. 32–41. https://doi.org/10.3141/1727-05.

34. Stevanovic, J., A. Stevanovic, P. T. Martin, and T. Bauer. Stochastic Optimization of Traffic Control and Transit Priority Settings in VISSIM. *Transportation Research Part C: Emerging Technologies*, Vol. 16, 2008, pp. 332–349. https://doi.org/10.1016/j.trc.2008.01.002.

35. Fang, C., and L. Elefteriadou. Development of an Optimization Methodology for Adaptive Traffic Signal Control at Diamond Interchanges. *Journal of Transportation Engineering*, Vol. 132, No. 8, 2006, pp. 629–637.

36. Stevanovic, A., J. Stevanovic, and C. Kergaye. Optimization of Traffic Signal Timings Based on Surrogate Measures of Safety. *Transportation Research Part C: Emerging Technologies*, Vol. 32, No. April 2016, 2013, pp. 159–178. https://doi.org/10.1016/j.trc.2013.02.009.

37. Gökce, M. A., E. Öner, and G. Isik. Traffic Signal Optimization with Particle Swarm Optimization for Signalized Roundabouts. *Simulation: Transactions of the Society for Modeling and Simulation International*, Vol. 91, No. 5, 2015, pp. 456–466. https://doi.org/10.1177/0037549715581473.

38. Matos, S. A., and A. B. Carvalho. Traffic Lights Signaling Optimization as a Many-Objective Optimization Problem. *Encontro Nacional de Inteligência Artificial e Computacional. Proceedings.*, 2016, pp. 421–432.

39. Leonard, J. D., and L. A. Rodegerdts. Comparison of Alternate Signal Timing Policies. *Journal of Transportation Engineering*, Vol. 124, No. 6, 1998, pp. 510–

520.

40. Abbas, M. M., H. A. Rakha, and P. Li. Multi-Objective Strategies for Timing Signal Systems under Oversaturated Conditions. *Proceedings of the IASTED International Conference on Modelling and Simulation*.

41. Singh, L., S. Tripathi, and H. Arora. Time Optimization for Traffic Signal Control Using Genetic Algorithm. *International Journal of Recent Trends in Engineering*, Vol. 2, No. 2, 2009, pp. 4–6.

42. Li, S., Y. Li, B. Fu, and W. Dang. Study on Simulation Optimization of Dynamic Traffic Signal Based on Complex Networks. *Procedia Engineering*, Vol. 137, 2016, pp. 1–10. https://doi.org/10.1016/j.proeng.2016.01.228.

43. Leonard, J. D., and L. A. Rodegerdts. Comparison of Alternate Signal Timing Policies. *Journal of Transportation Engineering*, Vol. 124, No. 6, 1998, pp. 510–520.

44. Rabbani, E. K., and G. Bullen. Marginal Delay: New Measure for Quality of Service at Signalized Intersections. *Transportation Research Record 1802*, No. 2, 2002, pp. 142–145. https://doi.org/10.3141/1802-05.

45. Li, X., G. Li, S.-S. Pang, X. Yang, and J. Tian. Signal Timing of Intersections Using Integrated Optimization of Traffic Quality, Emissions and Fuel Consumption: A Note. *Transportation Research Part D: Transport and Environment*, Vol. 9, 2004, pp. 401–407. https://doi.org/10.1016/j.trd.2004.05.001.

46. Deb, K., A. Pratap, S. Agarwal, and T. Meyarivan. A Fast and Elitist Multiobjective

Genetic Algorithm: NSGA-II. *IEEE Transactions on Evolutionary Computation*, Vol. 6, No. 2, 2002, pp. 182–197.

47. Deb, K., and H. Jain. An Evolutionary Many-Objective Optimization Algorithm Using Reference-Point-Based Nondominated Sorting Approach , Part I : Solving Problems With Box Constraints. *IEEE Transactions on Evolutionary Computation*, Vol. 18, No. 4, 2014, pp. 577–601.

48. Unal, M., G. Warn, and T. W. Simpson. Introduction of a Tradeoff Index for Efficient Trade Space Exploration. *Proceedings of the ASME 2015 International Design Engineering Technical Conferences & Computers and Information in Engineering Conference. Proceedings.*, 2015, pp. 1–12.

49. Unal, M., G. P. Warn, and T. W. Simpson. Quantifying Tradeoffs to Reduce the Dimensionality of Complex Design Optimization Problems and Expedite Trade Space Exploration. *Structural and Multidisciplinary Optimization*, Vol. 54, No. 2, 2016, pp. 233–248. https://doi.org/10.1007/s00158-015-1389-7.

50. Rakha, H., Y.-S. Kang, and F. Dion. Estimating Vehicle Stops at Under-Saturated and Over-Saturated Fixed-Time Signalized Intersections. *Transportation Research Record 1776*, 2001, pp. 128–137. https://doi.org/10.3141/1776-17.